Bulk and molecular-level composition of primary organic aerosol from wood, straw, cow dung, and plastic burning

Jun Zhang[1], Kun Li[1,a], Tiantian Wang[1], Erlend Gammelsæter[1,b], Rico. K. Y. Cheung ~~Ka Yuen Cheung~~[1], Mihnea Surdu[1], Sophie Bogler[1], Deepika Bhattu[2], Dongyu S. Wang[1], Tianqu Cui[1], Lu Qi[1], Houssni Lamkaddam[1], Imad El Haddad[1], Jay G. Slowik[1], Andre S. H. Prevot[1], David M. Bell[1]

[1]Laboratory of Atmospheric Chemistry, Paul Scherrer Institute, Villigen, 5232, Switzerland

[2]Department of Civil and Infrastructure Engineering, Indian Institute of Technology Jodhpur, 342037, India

[a]now at: Environmental Research Institute, Shandong university, Qingdao, 266237, China

[b]now at: Department of Chemistry, Norwegian University of Science and Technology, Trondheim, 7491, Norway

Correspondence to: Andre S. H. Prevot (andre.prevot@psi.ch) and David M. Bell (david.bell@psi.ch)

Field Code Changed

Abstract. During the past decades, the source apportionment of organic aerosol (OA) in the ambient air has been improving substantially. The database of source retrieval model resolved mass spectral profiles for different sources has been built with the aerosol mass spectrometer (AMS). However, distinguishing similar sources (such as wildfires and residential wood burning) remains challenging, as the hard ionization of AMS mostly fragments compounds and therefore cannot capture the detailed molecular information. Recent mass spectrometer technologies of soft ionization and high mass resolution have allowed for aerosol characterization at the molecular formula level. In this study, we systematically estimated the emission factors and characterized the primary OA (POA) chemical composition with the AMS and the extractive electrospray ionization time-of-flight mass spectrometer (EESI-TOF) for the first time from a variety of solid fuels, including beech logs, spruce and pine logs, spruce and pine branches and needles, straw, cow dung, and plastic bags. The emission factors of organic matter estimated by AMS and hydrocarbon gases estimated by the total hydrocarbon analyzer are 16.2 ± 10.8 g kg^{-1} and 30.3 ± 8.5 g kg^{-1} for cow dung burning, which is generally higher than that of wood (beech, spruce, and pine), straw, and plastic bags burning (in the range from 1.3 to 6.2 g kg^{-1} and 2.8 to 9.4 g kg^{-1}). The POA measured by the AMS shows that the f_{60} (mass fraction of m/z 60) varies from 0.003 to 0.04 based on fuel types and combustion efficiency for wood (beech, spruce, and pine) and cow dung burning. ~~The contribution of some polycyclic~~ Polycyclic aromatic hydrocarbons are observed in the burning emission~~is linked to burning fuels~~. On molecular level, the dominant compound of POA from wood, straw, and cow dung is $C_6H_{10}O_5$ (mainly levoglucosan), contributing ~7% to ~30% of the total intensity, followed by $C_8H_{12}O_6$ with fractions of ~2% to ~9%. However, as they are prevalent in all burns of biomass material, they cannot act as tracers for the specific sources. By using the Mann-Whitney U test among the studied fuels, we find specific potential new markers for these fuels from the measurement of the AMS and EESI-TOF. Markers from spruce and pine burning ~~could be~~are likely related to resin ~~and conifer needle-related~~acids (e.g. compounds with $20-21$ carbon atoms). The product from pyrolysis of hardwood lignins is found especially in beech logs burning. Nitrogen-containing species are selected markers primarily for cow dung open burning. These markers in the future will provide ~~important~~ support for the source apportionment.

Key words: AMS, EESI-TOF, biomass burning, source apportionment, markers

1 Introduction

Emissions from combustion are a major source of primary organic aerosol (POA), black carbon (BC), inorganic aerosol, and inorganic / organic gases (Andreae, 2019; Bond et al., 2007). After being emitted to the atmosphere, volatile organic compounds (VOCs) can further react to form lower volatility components and generate secondary organic aerosol (SOA). The primary emissions and their subsequent transformations have significant implications for air quality, climate, and human health (Chen et al., 2017). Accordingly, a large number of laboratory and field measurements have been carried out to disentangle the roles of burning-induced aerosols in polluted areas.

Solid fuel combustion is a major source of air pollution in many places over the world. In Southeast Asia, haze events are mainly attributed to the wildfires, agricultural waste burning, and peatland fires (Adam et al., 2021). In developing regions, such as India, more than half of households use inefficient stoves for cooking, burning solid fuels such as firewood, charcoal, crop residues, and cow dung (Census of India, 2011). This contributes to poor household air quality, chronic and acute respiratory diseases, and even premature death (Smith et al., 2014). Plastic burning has been estimated to contribute 13.4% of fine particulate matter ($PM_{2.5}$) yearly in India (Gadi et al., 2019), 6.8% in wintertime in China (Haque et al., 2019), and 2% to 7% in wintertime in the US (Islam et al., 2022). The toxic pollutants released from plastic burning, including olefins, paraffin, and polycyclic aromatic hydrocarbons, can cause respiratory irritation, and carcinogenic and mutagenic effects (Pathak et al., 2023). The extent to which primary particulate matter adversely affects health is source-dependent. Recent studies have shown that biomass burning-related particles has have been linked to reactive oxygen species and oxidative stress, increasing the risks of cardiovascular diseases (Daellenbach et al., 2020; De Oliveira Alves et al., 2017; Tuet et al., 2019). Therefore, identifying the sources of aerosols is essential for assessing health risks and developing mitigation strategies.

Organic aerosol (OA) source apportionment has been widely studied using receptor models, e.g. positive matrix factorization (PMF), with OA composition characterized by an aerosol mass spectrometer (AMS) or aerosol chemical speciation monitor (ACSM). Many studies have successfully resolved source-related factors, for example, hydrocarbon-like OA (HOA), oxygenated OA (OOA), biomass burning OA (BBOA), coal combustion OA (CCOA), and so on, via PMF (Chen et al., 2021; Huang et al., 2014; Ng et al., 2010; Tobler et al., 2020; Wang et al., 2019; Crippa et al., 2014). The identification and validation of resolved factors rely strongly upon the spectral characteristics of source emissions. For example, hydrocarbon ion series $C_nH_{2n+1}^+$ and $C_nH_{2n-1}^+$, e.g. $C_4H_9^+$ at m/z 57 and $C_3H_5^+$ at m/z 41, are often referenced as tracers for HOA (Mohr et al., 2012), while $C_2H_4O_2^+$ at m/z 60 is the main marker for wood and other biomass burning, as $C_2H_4O_2^+$ is a characteristic major fragment of anhydrosugars (e.g. levoglucosan) produced from cellulose pyrolysis (Alfarra et al., 2007). However, achieving finer separation and interpretation of sources within one of the OA categories mentioned above from highly mixed aerosols in the environment remains challenging, because the laboratory mass spectral profile database of primary emissions is limited and the potential molecular specificity is impeded by intensive fragmentation in the AMS and ACSM.

To minimize the loss of the molecular information from fragmentation, soft ionization and novel sampling techniques have been deployed to measure the chemical composition of particles in greater detail. A thermal desorption aerosol gas chromatograph (TAG) coupled to a AMS has been used and provided the molecular characterization of OA and SOA (Bertrand et al., 2018). The filter inlet for gases and aerosols (FIGAERO) measures molecular composition of OA via thermal desorption coupled to a chemical-ionization mass

78   spectrometer (Lopez-Hilfiker et al., 2014). Nonetheless, thermal decomposition can occur during the thermal
79   desorption process (Stark et al., 2017), causing potential artifacts and hindering the identification of components.
80   Liquid chromatography mass-spectrometer can avoid thermal desorption and separate mixtures including isomers
81   based their chemical affinity with the mobile and stationary phases (Zhang et al., 2021). However, it requires pre-
82   treatment of samples which could introduce artefacts and lowers the time resolution. An extractive electrospray
83   ionization time-of-flight mass spectrometer (EESI-TOF) has been recently developed for online OA measurement
84   with generally insignificant decomposition or fragmentation (Lopez-Hilfiker et al., 2019). As a result, it provides
85   a molecular-level (i.e., molecular formula determination) mass spectrum with a time resolution of seconds.
86   Consequently, improved real-time investigations of chemical composition in chamber experiments (Surdu et al.,
87   2023; Bell et al., 2022) and SOA source apportionment in the field measurement (Tong et al., 2021; Kumar et al.,
88   2022; Qi et al., 2022) became possible. Thus far, a detailed study of primary emissions from complex sources, e.g.
89   combustion, has not yet been conducted with the EESI-TOF, which necessitates the measurement to fully utilize
90   the chemical resolution capabilities of EESI-TOF for characterizing mass spectra and supporting the source
91   apportionment in the field.
92   In this work, we systematically characterize the POA composition using both AMS and EESI-TOF from a variety
93   of burning fuels from both residential stoves (beech logs and a mixture of spruce and pine logs) and open
94   combustion (spruce and pine branches and needles, straw, cow dung, and polyethylene plastic bags). The emission
95   factors of trace gases are presented and possible molecular markers for the burning fuels in this study are discussed.
96   This work allows for a better understanding of the POA chemical composition emitted from different burning
97   sources, and provides important reference spectra for source apportionment, and potential markers to use to assess
98   the importance of different biomass burning sources.

99   **2 Materials and methods**

100 **2.1 Experimental setup and instrumentation**

101 A total of 36 burning experiments were conducted using 6 different types of burning materials, including beech,
102 spruce, pine, straw, cow dung, and plastic bags. Beech logs, spruce and pine logs, fresh spruce and pine branches
103 and needles, as well as straw were sourced from a local forestry company in Würenlingen, Switzerland. Cow dung
104 cakes (made of cow dung and straw) were collected from Goyla dairy, Delhi, India, and polyethylene plastic bags
105 were bought in Delhi, India. To represent residential burning, logs of (1) beech and (2) spruce and pine were
106 burned separately in a stove (Bruns et al., 2017). Agricultural waste combustion and forest fires were respectively
107 represented by burning (1) straw and (2) a mixture of fresh branches and needles of spruce and pine in an open
108 stainless steel cylinder (65 cm in diameter and 35 cm in height). Finally, the half-open stove (e.g. angithi) and
109 waste burning in India and some other areas (Fleming et al., 2018), respectively, were represented by burning (1)
110 cow dung cakes and (2) plastic bags on top of the stainless steel cylinder, with the fuel resting on a mesh steel
111 plate. The experimental setup is shown in Figure S1. The fuels were ignited with fire starters / kindling and the
112 emissions were pulled into either a chimney (for stove burning) or a hood (for open burning). After starters /
113 kindling burnt away (~3 to 10 min. after ignition), the emissions were introduced into a stainless steel holding
114 tank (1 m^3) through stainless steel sampling lines heated to 180 °C and passing through an ejection dilutor (DI-
115 1000, Dekati Ltd.) with a dilution ratio of ~10. The holding tank is a stainless steel container (1 m^3) used to store

116 emissions. It is also designed for averaging the emissions at different combustion efficiency in order to fully
117 characterize the emission in the real ambient. The emissions were injected into the holding tank for 10 to 30 min,
118 depending on the emission source. Typically, the injection was stopped when the measured POA concentration
119 was above ~20 μg/m^3 after ~60 times dilution in the sampling lines. In different burning experiments, POA
120 concentrations in the holding tank varied between 1 to 5 mg m^{-3} prior to sampling line dilution. The holding tank
121 was flushed overnight with clean air before each experiment, ensuring the background particle concentrations
122 were less than 10 #/cm^3.
123 The emissions were delivered from the holding tank to sampling instruments via stainless steel lines (6 mm O.D.)
124 for particles and via Teflon lines (6 mm O.D.) for gases. Gas analyzers were used for monitoring the concentration
125 of CO (Horiba APMA-370), CO_2 (LI-COR LI-7000), and total hydrocarbon (THC, including methane) and
126 methane (Horiba APHA-370). Particle concentrations were measured using a scanning mobility particle sizer
127 (SMPS, model 3938, TSI) scanning a range of 16 to 638 nm. An aethalometer (AE 33, Magee Scientific) was
128 used to retrieve the concentration of equivalent BC (eBC). A long time-of-flight aerosol mass spectrometer
129 (LTOF-AMS, Aerodyne Research, Inc.) with a mass resolution of ~5000 over the range of m/z 100 to m/z 450
130 was deployed for online, non-refractory particle characterization and a subset of experiments were performed with
131 high-resolution time-of-flight AMS (HTOF-AMS, Aerodyne Research, Inc.) with a mass resolution of ~2000 over
132 the range of m/z 100 to m/z 450. The aerosols sampled by both the SMPS and AMS were dried with a Nafion
133 dryer (Perma Pure). The aerosol was continuously sampled by the AMS through a 100 μm critical orifice and
134 focused by PM_1 aerodynamic lens. Therefore, the class of the PM in this study belongs to PM_1. Mass spectra of
135 positive ion fragments (m/z 10 to 400) were obtained with a TOF mass spectrometer and were analyzed with the
136 software SQUIRREL (SeQUential Igor data RetRiEvaL) v.1.63 and PIKA (Peak Integration by Key Analysis)
137 v.1.23 for the IGOR Pro software package (Wavemetrics, Inc.). A detailed description of AMS can be found in
138 Decarlo et al. (2006).
139 EESI-TOF was deployed for a real-time and molecular-level (i.e., molecular formula) measurement of OA with
140 minimal analyte fragmentation or decomposition (Lopez-Hilfiker et al., 2019). Before entering the EESI-TOF,
141 the aerosol passes through an activated charcoal denuder to remove gas-phase species. The aerosol intersects a
142 spray of charged droplets generated by an electrospray probe. Particles coagulate with the electrospray (ES)
143 droplets, and water-soluble compounds are extracted into the solvent and then ionized via the Coulomb explosion
144 mechanism as the droplets evaporate. 100 ppm sodium iodide (NaI) in pure water (MilliQ) was used as the
145 electrospray solution, resulting in the formation of [M + Na]$^+$ (M is the analyte) adduct in the positive ionization
146 mode. The EESI-TOF mass analyzer achieved a mass resolution of ~10000 at m/z 173 and 11000 at m/z 323. The
147 EESI-TOF operated with a time resolution of 1 s, and alternated 1.5 min of background measurements (in which
148 the sampled air passes through a high efficiency particulate air (HEPA) filter to remove particles) with 3.5 min of
149 direct sampling. These data were pre-averaged to 5 s for further analysis. Ions are only considered as signals from
150 emissions when their intensity difference between the particle measurement and the corresponding background
151 measurement periods were 1.9 times bigger than the propagated standard errors over the measurement cycle. For
152 those selected ions, their mass flux to the detector was calculated as Equation 1:

$$Mass_x = \frac{I_x \times MW_x \times 10^{18}}{N_a} \qquad \qquad \textbf{\textit{Equation (1)}}$$

153

where $Mass_x$ and I_x are respectively the mass flux (attograms per second, ag s^{-1}) and the ion flux of (counts per second, cps) of a group of detected ions with the same molecular weight. MW_x is the molecular weight of x (with the mass of the charge carrier, typically Na$^+$, removed)–. N_a is Avogadro's number. To assist with the peak identification, filters were collected from emissions and were analyzed with an ultrahigh-resolution mass spectrometer (Orbitrap). The Orbitrap (Orbitrap Exploris 120, Thermo Fischer) has a mass resolving power of 140000 at m/z 200, and was operated in positive mode scanning from m/z 50 to 450.

2.2 Data analysis

The emission factor (EF) of species i was calculated using the carbon mass balance method (Radke and Ward, 1993), expressed in the unit of g kg $^{-1}$, as shown in Equation 2.

$$EF_i = \frac{m_i \cdot W_C}{\Delta CO + \Delta CO_2 + \Delta THC + \Delta OC + \Delta BC} \qquad \textit{Equation (2)}$$

where ΔCO, ΔCO_2, ΔTHC, ΔOC, and ΔBC are the background-corrected carbon mass concentrations of CO, CO_2, THC, OC (organic carbon), and BC. OC was calculated from the ratio of organic aerosol and the ratio of organic mass (OM) to OC (OM/OC) measured by AMS (Canagaratna et al., 2015). m_i is the mass concentration of species i. W_C is the carbon mass fraction of the burning fuel. The W_C was reported 0.46 for wood (Bertrand et al., 2017), 0.45 for straw (Li et al., 2007), 0.45 for cow dung (Font-Palma, 2019), and 0.84 for plastic bags (Li et al., 2001). In experiments, where BC is not available, the sum of OC and BC is considered equal to the particulate matter (PM) determined by SMPS. The effective density of particles applied in the SMPS is determined by comparing mass and volume distributions from the AMS and SMPS (Bahreini et al., 2005). The densities could be underestimated because of the non-spherical shape of particles, especially particles from plastic bags burning mainly due to the high contribution of BC. As the contribution of particles to the total carbon is much smaller than the gases, these two methods have little differences calculating the denominator in Equation 2. Therefore, the EFs of CO, CO_2, and THC are consistent using both methods. However, it could be important for calculating the EFs for particulate species because of the possible discrepancy between the mass measured by the SMPS and AMS arising from, for example, the particle size and effective density. Additionally, the OM/OC acquired by the AMS also would add uncertainty when converting OM to OC because the high range of m/z without peak fitting is not included in OM/OC. More comparison is discussed in Sect. 3.1.

The combustion condition was characterized by the modified combustion efficiency (MCE, Equation 3) (Ward and Hardy, 1991). When the MCE is higher than 0.9, the combustion is considered as predominantly flaming. When the MCE is lower than 0.85, it is dominated by smoldering.

$$MCE = \frac{\Delta CO_2}{\Delta CO + \Delta CO_2} \qquad \textit{Equation (3)}$$

2.3 Identification of potential markers

The identification of potential markers for emissions was performed by Mann-Whitney U test (Mann and Whitney, 1947; Wilcoxon, 1945) which has been applied in many fields and for the current study has the advantage that it does not require a large volume of normally distributed samples (Rugiel et al., 2021; Tai et al., 2022). It tests the null hypothesis that the two population medians are equal against the alternative hypothesis that the two populations are not equal. When the p-value is smaller than the significance level of 0.1, the median of the tested

188 sample is significantly high or low in the two-tailed test. Ions from a class of fuel that satisfy the pairwise

189 comparison test between one fuel j and other types of fuels were considered to be significantly high-fraction or

190 low-fraction ions in the fuel j and therefore have the potential as markers for the fuel j. The fold change (FC) of

191 ion i in the fuel j was calculated as the Equation 4, where the $f_{i,j}$ is the fraction of ion i in the mass spectra profiles

192 of the fuel j, and $f_{i,other}$ is the average fraction of ion i in the mass spectra from the other fuels.

$$FC_{i,j} = \frac{f_{i,j}}{f_{i,other}}$$ *Equation (4)*

193 **3 Results and discussion**

194 **3.1 Emission factors from combustion**

195 The average EFs of CO, CO_2, THC, PM, OM, and eBC, as well as the MCE values of the 6 types of burning are

196 shown in Table 1, and the EFs and MCE values for each experiment are presented in Table S1.

197 The average MCE values depend on fuel types, with the lowest values of 0.87 ± 0.03 (average ± 1 σ) observed

198 from cow dung open burning and the highest values of 0.98 ± 0.02 from plastic bags open burning, consistent

199 with smoldering combustion for cow dung and flaming/melting processes for plastic bags. Accordingly, cow dung

200 had the highest average CO EF (92.3 ± 27.4 g kg^{-1}) and the lowest CO_2 EF (1366.2 ± 88.4 g kg^{-1}), and vice versa

201 for plastic bags. The strong relationship between the MCE and some EFs is also true for the THC. In general,

202 lower the MCEs correspond to higher THC EFs within a given class of burning fuel. Taking straw burning as an

203 example, as shown in Table S1, the EFs of THC vary from 0.7 to 39.3 g kg^{-1}, with the MCE varying from nearly

204 1.00 to 0.89 correspondingly, resulting the high standard deviation of the EFs. These EFs of gases are comparable

205 with the reported EFs from the ~~literatures~~literature under similar conditions (Hennigan et al., 2011; Fang et al.,

206 2017; Bertrand et al., 2017).

207 The average EFs of PM is in the range of 3.1 to 16.6 g kg^{-1}. In general, the PM emitted from cow dung is dominated

208 by OM, and the eBC is minor. For beech logs and straw, the OM EF is around 3 times higher than the eBC EF.

209 Noticeably, the emission of PM from plastic bags is not very high (3.0 g kg^{-1}), but the EF of OM and eBC is

210 similar (1.5 g kg^{-1} v.s. 1.0 g kg^{-1}). Note that when eBC data is not available, the sum of OC and BC in the

211 denominator in Equation 2 is assumed to be equal to the PM measured by the SMPS. Table S1 lists the comparison

212 of EFs for particulate species where possible. For the experiments of cow dung open burning and plastic bags

213 open burning, the EFs are consistent using both methods with the difference of PM EF < 6%, and on average less

214 than 15% for OM EF. However, for some beech logs stove burning experiments (BS3 and BS4), the effective

215 density required in the calculation is not available, and the average density of other beech logs in this study is

216 used. This results in some variance between these two methods. In general, the EFs of PM, OM, and BC agree

217 well with some previous literature (Fang et al., 2017; Goetz et al., 2018; Tissari et al., 2008). Nevertheless, the

218 reported EF values are highly dependent on the burning method (e.g. stove type) and combustion efficiency

219 (Bertrand et al., 2017). Additionally, the reported EFs for plastics vary ~~a lot~~substantially with their composition,

220 and the EF of the pure PE plastic bags are not often reported (Jayarathne et al., 2018; Wu et al., 2021; Hoffer et

221 al., 2020).

Formatted: Font color: Auto

6

3.2 Chemical composition of POAs from combustion

3.2.1 Chemical composition of POAs measured with the AMS

The chemical composition of POAs of burning emissions ~~are~~ is characterized with the AMS and EESI-TOF simultaneously. As shown in Figure 1, the average mass spectra from m/z 10 to 120 measured with AMS is grouped into C_xH_y, $C_xH_yO_1$, $C_xH_yO_{2+}$, ~~and~~ $C_xH_yN_z$, and $C_xH_yO_{1+}N_z$ families based on their elemental composition. ~~The mass spectrum of plastic bags burning is not shown because considerable $C_xH_yO_x$ family was observed (23%), but it is more likely from the emission remaining in the tubing of other fuels than from the plastic bags given the fact that polyethylene is the main component of it.~~ In all the POAs, the C_xH_y-family is the most abundant group, mainly from ions at m/z 29, 39, 41, 43, 55, 57, 67, and 69 originating primarily from hydrocarbon compounds, with the biggest contribution ~~for~~ from plastic bags (92%), followed by cow dung (~~72~~70%) and straw (~~62~~61%), generally higher than that of wood (beech, spruce, and pine, 48% to ~~55~~54%) burning. The $C_xH_yO_{2+}$ and $C_xH_yO_1$ families are the second largest compositions, with major ions at m/z 28, 29, 43, 44, and 60, which are higher in wood and straw emissions compared to cow dung. Among these ions, the mass fractions of m/z 44 (f_{44}, mostly CO_2^+), mass fraction of m/z 43 (f_{43}, mostly $C_2H_3O^+$ and $C_3H_7^+$), and mass fraction of m/z 60 (f_{60}, mostly $C_2H_4O_2^+$) have the largest impact on the oxidation state of the aerosol. The fragment $C_2H_4O_2^+$ at m/z 60 is widely used as a levoglucosan related marker for biomass burning and is most prominent in the wood burning emissions compared to the other burning fuels. Figure 2a shows that the POAs in this study are at the left bottom of the ambient OOA range (Ng et al., 2010) in the f_{44} vs f_{43} plot, indicating the POA is less oxygenated, which is consistent with previous studies (Hennigan et al., 2011; Fang et al., 2017; Xu et al., 2020). As shown in Figure 2b, the f_{60} for the biomass source studied is greater than the background level (Cubison et al., 2011), suggesting the f_{60} filter (f_{60} = 0.003) in the ambient is unlikely to miss biomass combustion. The contribution of f_{60} relates to the burning fuel types and the combustion efficiency. For example, the f_{60} from wood burning ranges from 0.02 to 0.04, generally higher than that of cow dung. The f_{60} of straw open burning is distributed from below 0.01 to 0.025, resulting from the low to high MCE values correspondingly. The pie charts in Figure 1 indicate that the N-containing fragments from AMS are mainly from $C_xH_yN_z$ and $C_xH_yO_{1+}N_z$ family and ~~it is~~ they are the largest in the emission of cow dung open burning (~~~~3~~4.3~~%) and followed by straw (3.4~~2~~%), while the wood is relatively minimal ($\leq$ 1%) (Stockwell et al., 2016). The nitrogen in organonitrates would appear mainly at fragments of NO^+ and NO_2^+. However, the NO^+ and NO_2^+ originating from organonitrates are estimated almost 20 times smaller than $C_xH_yN_z$ family in cow dung burning using the NO^+ and NO_2^+ ratio between inorganic nitrates and organonitrates (Farmer et al., 2010), suggesting their contributions are minor to organic nitrogen.

In the region from m/z 120 to 450 as shown in Figure ~~S2~~S3, polycyclic aromatic hydrocarbons (PAHs) are observed. Based on the spectra of laboratory standards (Dzepina et al., 2007; Aiken et al., 2007), parent ions at m/z 226,~~239,~~ 252, 276, 300, and 326 correspond respectively to ~~$C_{18}H_{10}$ (benzo[ghi]fluoranthene and cyclopenta[cd]pyrene)$C_{19}H_{12}$ (methylbenzofluoranthene),~~ $C_{20}H_{12}$ (benzofluoranthene and benzopyrene), $C_{22}H_{12}$ (indenopyrene and benzoperylene), $C_{24}H_{12}$ (coronene), and $C_{26}H_{14}$ (dibenzoperylene). The fragment of m/z 239 could ~~come~~be ~~be from~~ from methylbenzo[ghi]fluoranthene ($C_{19}H_{12}$) (Dzepina et al., 2007; Ji et al., 2010) or a fragment of dehydroabietic acid which has been found in fresh pine resin (Colombini et al., 2005). The m/z 219 and m/z 285 also could arise from the fragmentation of retene and dehydroabietic acid, respectively, which also can be derived from conifer resin (Dzepina et al., 2007; Jen et al., 2019; Zetra et al., 2016). These ions contribute 0.69% $\pm$ 0.14% and 0.66% $\pm$ 0.11% respectively to the total POA of the spruce and pine branches and needles open burning as

262 well as spruce and pine logs stove burning, which is distinct from straw (0.36% ± 0.13%), beech logs (0.34% ±
263 0.14%), and cow dung (0.25% ± 0.13%). Not many PAHs are observed with the AMS for the plastic bags. ~~The~~
264 ~~lower bound of the contribution of these ions for plastic bags is estimated as 0.57% ± 0.37%.~~ The difference for
265 the observed PAH contribution is mainly caused by the burning material, i.e., the precursor of PAHs, such as
266 lignin, single-ring compounds, and aliphatic hydrocarbons. The burning of PE has lower yield of PAHs than lignin
267 (Zhou et al., 2015), resulting in the lower PAH contribution in the burning of polyethylene plastic bags.~~Of~~
268 ~~particular note is the series of high intensity ions at m/z >350 in emissions from the plastic bags open burning.~~
269 ~~Reference mass spectra of PAHs at higher mass-to-charge ratio (> m/z 350) is not available so far, but from the~~
270 ~~PAH pattern of spikes spacing ~24   26 amu, we speculate that this series does come from a series of high~~
271 ~~molecular weight PAHs.~~

Formatted: Font color: Auto

3.2.2 Chemical composition of POAs measured with the EESI-TOF

273 The EESI-TOF provides an important complement to the highly fragmented mass spectra generated by the AMS,
274 where intact compounds measured by the EESI-TOF from m/z 100 to 400 without assuming specific response
275 factors toward each molecular formula are shown in Figure 3. The mass spectrum of plastic bags in not shown
276 because the EESI-TOF is insensitive to hydrocarbons because of their low solubility in the electrospray and low
277 affinity for Na$^+$. The bin of compounds containing O/C greater than 0.7 has the largest and similar contribution in

Formatted: Superscript

278 wood burning (29.9% to 31.5%), and it is slightly smaller in straw (25%) and cow dung (20.1%). O/C smaller
279 than 0.15 contributes 15.3% to 18.8% in spruce and pine which is similar to the fraction in cow dung (13.5%) but
280 much higher compared to beech logs (4.7%) and straw (8.8%), mainly due to the greater contribution of
281 compounds with carbon numbers in the range of 18 to 21. Cow dung has a slightly lower fraction of low-H/C and
282 a slightly higher fraction of high-H/C comparing to other fuels studied.
283 As shown in the pie charts in Figure 3, the $C_xH_yO_z$-family is the main group measured by the EESI-TOF with
284 contribution from 80% to 97%. The N-containing species have the highest contribution (19.6%) in the POA from
285 cow dung open burning, which is much higher than other fuels in this study (2.5% to 8.9%). Of the N-containing
286 species in cow dung POA 95% contain one nitrogen atom and are in a wide range of carbon number between 5
287 and 22.~~.~~ They are ~~with~~ mainly in the O/C range of < 0.15 to 0.5 and the H/C from 1.2 to > 1.7 (Figure ~~S3~~S4). The
288 degree of unsaturation, calculated from the ratio of the double-bond equivalent to the number of carbons (DBE/C).
289 The difference in all the studied POAs is not major (Figure ~~S4~~S5).
290 On molecular level, $C_6H_{10}O_5$ (m/z 162.0523) is most abundant in wood combustion (20.3% ± 6.1%), is less
291 pronounced in straw (15.0~~%~~% ± 7.9%) and even less so in cow dung emissions (9.9% ± 5.4%) (Figure 2c). It
292 could be mainly assigned to levoglucosan (or similar dehydrated sugars) which is formed from the pyrolysis of
293 cellulose and hemicellulose (Simoneit, 2002). The second most abundant species presented in the POAs is
294 $C_8H_{12}O_6$ (m/z 204.0628) in this study, contributing between 2 and 9%. It has been observed from the primary
295 biomass burning emissions in the laboratory and ambient studies (Kumar et al., 2022; Kong et al., 2021). In
296 addition, compounds with 18 and 20 carbon atoms are rich in many fuel types, particularly in spruce and pine
297 burning emissions, and are notably minimal in beech logs.
298 The O/C (calculated as the ratio of total oxygen to total carbon) of the POAs from 5 types of burning measured
299 by the EESI-TOF is 0.32 ± 0.07~~–~~ to 0.41 ± 0.02, which is higher than that of the AMS (0.16 ± 0.07 to~~–~~ 0.37±
300 0.08). The difference likely occurs because the EESI-TOF is insensitive to species with low water solubility and/or

301   low affinity for Na^+ (e.g., hydrocarbons including polyaromatic hydrocarbons). This ~~may also~~will contribute to

302   an underestimation of H/C. The total nitrogen-to-total carbon ratio (N/C) of cow dung measured by EESI-TOF is

303   0.019, which is slightly higher than that in the AMS measurements (0.015). This could be partially because of the

304   difference in EESI sensitivity to the N-containing molecules. Another reason is that the total carbon from POA

305   measured by the EESI-TOF is smaller, again consistent with the absence of non-water-soluble substances or

306   molecules that do not bind to Na^+.

3.3 Literature ~~Common~~ markers for solid-fuel combustion

308   Levoglucosan and dehydrated sugars having the molecular formula $C_6H_{10}O_5$ are commonly used as tracers for

309   biomass burning. A range of values for the fraction of $C_6H_{10}O_5$ is observed both for the same fuel type under

310   different burning conditions and for different fuel types, as seen in Figure 2c. Thus, $C_6H_{10}O_5$ is a good untargeted

311   marker for biomass burning, but cannot be used to determine the specific source (or type of combustible)

312   responsible for biomass burning emissions. Likewise, the $C_8H_{12}O_6$ is not a suitable marker for specific emission

313   sources, as it is prevalent in all burns of biomass material. Additionally, $C_8H_{12}O_6$ has been considered as a tracer

314   for terpene or syringol-derived SOA (Szmigielski et al., 2007; Yee et al., 2013), however our results suggest this

315   molecular formula is not a good marker for SOAs due to the strong contribution from biomass burning-derived

316   POA.

317   At a higher mass range, $C_{16}H_{32}O_2$ and $C_{18}H_{30,32,34}O_2$ are likely to be the common saturated and unsaturated fatty

318   acids corresponding to palmitic, linolenic, linoleic, and oleic acid, which are important structural components of

319   cells and ~~were~~ have been found in the emission of cooking, biomass burning, and cow dung (Simoneit, 2002;

320   Neves et al., 2009a; Neves et al., 2009b; Brown et al., 2021). The corresponding compounds for the $C_{20}H_{30}O_2$ and

321     $C_{20}H_{28}O_2$ are most likely resin acids (e.g., abietic acid and pimaric acid) and dehydroabietic acid which have been

322   specifically found in coniferous ~~wood species~~resin (Holmbom, 1977; Simoneit, 2002) and served as biomass

323   burning tracers (Simoneit et al., 1993; Liang et al., 2021). The $C_{20}H_{30,32,24}O_{2,3}$ have been found as diterpenoids

324   from the wood of Cunninghamia konishii (Li and Kuo, 2002). This plant species belongs to the class of Pinopsida,

325   which also includes spruce and pine.

326   These typical markers stated above are well-known, but due to their presence in more than one fuel, the

327   determination of different BB sources (or even biomass burning-derived POA) is challenging. For example,

328   scaling levoglucosan to total BB OM requires a priori knowledge of the BB source and burning condition (Favez

329   et al., 2010). Therefore, it is complicated to apply these markers in the source apportionment without comparison

330   to statistically rule out other possibilities.

3.4 Identification of potential markers for specific solid fuels

332   To investigate the feasibility of distinguishing differences between the combustion fuel sources based on the

333   measured species, the similarity of mass spectra acquired from each experiment by AMS and EESI-TOF is

334   assessed with Spearman's rank correlation coefficient (r), as shown in Figure 4. The calculation of Spearman's

335   coefficient is equivalent to calculating the Pearson correlation coefficient on the rank-ordered data, so it assesses

336   monotonic relationships for ions from two mass spectra. In the correlation matrix with the fragment ions from

337   AMS (Figure 4a), it is clear that the POAs from the same burning fuel strongly correlate. For instance, the average

338   correlation coefficients of the AMS POA MS for all experiments using the same fuel range from 0.84 to 0.95.

Formatted: Subscript

Formatted: Subscript

Formatted: Subscript

339　　When comparing different fuels, a strong correlation is also found between spruce and pine logs stove burning
340　　and spruce and pine branches and needles open burning (0.95 ± 0.02). This is mainly because these two types of
341　　burning are closely related (i.e., derived from the same plants), and therefore have similar chemical composition.
342　　The correlation weakened when comparing POAs from different materials (e.g., spruce – beech 0.77 ± 0.03,
343　　spruce – straw 0.76 ± 0.03, spruce – cow dung 0.75 ± 0.03).
344　　By contrast, the correlation coefficients based on the species from EESI-TOF are much lower among different
345　　burning fuels and even amongst the same fuel type (0.44 to 0.68). Noticeably, only a weak intra-fuel correlation
346　　is found for spruce/pine logs stove burning (0.44 ± 0.07), indicating that there are significant differences between
347　　experiments which are likely driven by burn-to-burn variability caused by differences in the combustion condition
348　　or variance of the fuel materials (e.g., with or without bark, amount of sap in the wood, etc.). Nevertheless, the
349　　variability between different fuels is clearly larger than the intra-fuel variability for the POAs. For example, the
350　　correlation between the cow dung and all the other fuels (average 0.27 ± 0.11) is significantly lower than that of
351　　among cow dung emissions (0.49 ± 0.16). This suggests that the EESI-TOF may be capable of distinguishing
352　　between different types of BB fuels.
353　　To perform a more detailed analysis and identify markers between the emissions, the Mann-Whitney U test (see
354　　Sect. 2.2) of the POAs from different fuels measured by AMS and EESI-TOF is conducted. Considering that both
355　　spruce and pine logs stove burning as well as spruce and pine branches and needles are similar fuel types and have
356　　a comparable POA composition in Figures 1 to 3, they were classified as the same fuel for this test. Results of the
357　　Mann-Whitney U test are presented in Figure 5, where we show the average $-\log_{10}$ of the p-value as a function of
358　　the $\log_2$ of the fold change (FC). Species having p-values less than 0.1 in the two-tailed test in all pairwise
359　　comparisons are considered to be significantly more prevalent or scarcer in a single fuel compared to all other
360　　fuels. These ions are represented as colored circles in Figure 5. If the species fail to meet the criterion one time or
361　　more than one time, those species will be shown as gray circles even though their average p-value might be lower
362　　than 0.1. A higher $-\log_{10}(p\text{-value})$ (i.e., a lower p-value) indicates a lower probability that the fractional medians
363　　of two species are equal. At the same time, a higher FC (Equation 4) indicates a higher abundance of the species'
364　　fractional contribution in the tested fuel compared to the average of all other fuels, deeming it more exclusive. In
365　　the case of beech logs as well as spruce and pine logs burning, the colored p-value is lower (higher $-\log_{10}(p\text{-value})$)
366　　in the dataset of AMS than that of EESI-TOF, suggesting the results from the AMS are more replicable. However,
367　　from the perspective of FC, its absolute value is around 2 to 4 times higher in the dataset of the EESI-TOF than
368　　that of the AMS. This shows that the potential markers selected from the EESI-TOF measurement are more unique,
369　　in some cases found only in the spectrum of a given source. On this ground, the AMS and EESI-TOF are potent
370　　complementary tools to provide separation and source apportionment of ambient OA, and to capture marker
371　　compounds. The selected potential markers, p-values, and fold changes are listed in Table S2 and Table S3 for
372　　EESI-TOF and AMS data, respectively.
373　　Mass defect plots of the selected marker compounds are visualized in Figure 6. Many more potential markers are
374　　identified from spruce and pine burning, as well as cow dung open burning, in comparison to beech and straw
375　　burning. As shown in Figure 6A with the AMS dataset, potential markers from C_xH_y and $C_xH_yO_z$-family have
376　　significantly higher fraction in the POA of beech logs than those in other fuels. By contrast, the selected markers
377　　for spruce and pine burning are more oxidized and mainly composed of $C_xH_yO_z$-family, which is consistent with
378　　its bulk chemical composition and relatively higher O/C. The main fragments CO^+ and CO_2^+ have higher

10

379   contributions in spruce and pine burning (also can be seen in Figure 1), but their FCs are not very high, which
380   means they are not exclusive in spruce and pine and therefore are not applicable as sole tracers in the complex
381   ambient air. Fragments from cow dung open burning have considerably higher contribution in C_xH_y-family and
382   N-containing families, but lower in oxygen-containing species, which also agrees with bulk chemical composition
383   characteristics.

384   Similarly, many marker compounds are determined in the measurement of EESI-TOF for spruce and pine burning
385   as well as cow dung open burning. Compounds with $20 - 21$ carbon atoms as shown in Figure 6B for spruce and
386   pine burning could be resin and conifer needle-related, such as $C_{20}H_{32}O_3$ (likely isocupressic acid) (Mofikoya et
387   al., 2020; Wiyono et al., 2006). However, $C_{20}H_{30}O_2$ mentioned in pre previous section with notable abundance is
388   not stably emitted in each spruce and pine burn. Therefore, it is not determined as a marker for spruce and pine.
389   Homologues of $C_{11}H_{12}(CH_2)_{0-3}O_7$ are also determined, of which $C_{14}H_{18}O_7$ could be picein which is an important
390   phenolic compound in the needles of spruce (Løkke, 1990). On the other hand, some compounds which are barely
391   present in the POA of spruce and pine burning, such as $C_{14}H_{28}(CH_2)_{0-3}O_2$ (likely saturated fatty acids), offers an
392   alternative perspective of exclusion method in source separation. Noticeably, while coniferyl alcohol ($C_{10}H_{12}O_3$)
393   is a major pyrolysis product from softwood (e.g., spruce) lignins (Saiz-Jimenez and De Leeuw, 1986) and has a
394   decent fractional contribution in POA of the spruce and pine burning, but its contribution in spruce and pine
395   burning is smaller than straw burning. Therefore, it is not recommended as a tracer when other biomass fuels are
396   present. For the hardwood (i.e., beech logs in this study), sinapyl alcohol ($C_{11}H_{14}O_4$) is one of the prominent
397   products from pyrolysis of lignins (Saiz-Jimenez and De Leeuw, 1986) and is conspicuous in our beech logs stove
398   burning. Interestingly, nitrogen-containing compound $C_{13}H_{17}NO_6$ is noted as a tracer for straw open burning, and
399   the nitrogen-containing fragments $C_3H_{8-9}N$ are also selected from the straw AMS analysis.

400   Cow dung is a clearly different fuel to other biomass fuels in this study, thus many markers are identified from
401   cow dung open burning. These potential markers have mostly nitrogen in chemical composition and with generally
402   higher FC. Many series of N-containing homologues are found, such as $C_{10}H_9NO_2$ and $C_{11}H_{11}NO_2$, which could
403   be likely assigned to the derivative of indole, i.e., indole acetic acid and indolepropionic acid respectively. Another
404   series of homologues is $C_9H_{11}NO_2$ and $C_{10}H_{13}NO_2$, which have been found especially in the emissions from cow
405   dung cook fire in India compared to brushwood cook fire (Fleming et al., 2018). Homologues without nitrogen
406   atoms in the chemical composition are also seen, for example, $C_{22}H_{42}(CH_2)_{0-2}O_2$, likely the homologues of erucic
407   acid which is a natural fatty oil mainly present in the Brassicaceae family of plants. Nevertheless, it is not very
408   surprising to see the biomass-related species as cows are herbivorous animals.

409   From the perspective of source-apportionment, ions that are primarily associated with a specific emission source
410   and exhibit minimal contribution from other sources can be considered as potent in use. To show the ability of
411   these markers for source separation, the contribution of two markers for the same source from Table S2 and Table
412   S3 that possess small p-value with high FC are plotted among studied fuels. As shown in Figure S6, these markers
413   measured by the AMS have relatively higher contribution in one specific fuel, which makes the fuel distinctive
414   from others. Nonetheless, one would need to coordinate with more tracers to draw a conclusive diagnosis because
415   the presence of these markers in other fuels. Given this scenario, the markers that have significantly low
416   contribution (FC < 1) in a specific fuel could shed the lights on. In contrast, markers observed from the EESI-
417   TOF is more robust for utilization as most of them are unique. As the markers listed in Table S2 and Table S3 are

418　many, we could not thoroughly discuss here. However, due to the limited fuel types, referencing more markers
419　can provide more confidence in source identification.
420
421　To the best of our knowledge, most of these markers are reported for the first time in POA emissions from the
422　studied fuels with the EESI-MS, which is becoming more commonly used in the measurement of atmospheric
423　aerosols. They could improve the refinement in source separation of fuels in biomass burning. Replicability and
424　specificity are two important criteria for tracers. The p-value being less than 0.1 in the two-tailed test can ensure
425　the stability of the shown results. The FC tells the degree of specificity of markers of one fuel in the presence of
426　other fuels. If the p-value criterion is satisfied and the FC is large, the presence of this marker can directly lead us
427　to the emission source. On the other hand, if the FC is less than 1, the detection of this compound can decisively
428　exclude the related source after verifying this isn't due to a detection limit issue. However, if the FC is in-between,
429　more caution is needed because these compounds don't have a distinctive fraction in that fuel compared to other
430　fuels, but could have a relatively fixed ratio compared to other markers.

431　**4 Conclusions**

432　In this study, we conducted 36 burning experiments to simulate typical solid fuel combustion emission, including
433　residential burning (beech or spruce and pine logs stove burning), wildfire (spruce and pine braches and needles
434　open burning), agriculturaland agricultural residue in field burning (straw open burning), cow dung open burning,
435　and plastic bags open burning. The emission factors of CO, CO_2, THC, PM, OM, and BC were determined. The
436　chemical composition of particles emitted from the combustion processes was comprehensively characterized
437　using the AMS and the EESI-TOF, and the chemical composition of the particles measured by the two instruments
438　were compared. These are the first direct measurements of these source profiles with the EESI-TOF. The utility
439　of traditional markers are discussed, and new potential markers were identified using the Mann-Whitney U test.
440　The EFs of CO and THC are generally higher during the low combustion efficiency, and the opposite for the EF
441　of CO_2. The highest EF of PM (16.6 ± 10.8 g kg^{-1}) is from cow dung open burning which is mostly OM (16.2 ± 10.8
442　g kg^{-1}), but for residential and plastic bags burning, the eBC accounts for ~30% of the total PM. The organics
443　measured by the AMS show that the wood (beech, spruce, and pine) burning emission has a relatively higher
444　abundance of $C_xH_yO_z$ fragments, while straw and cow dung burning emissions are dominated by C_xH_y fragments
445　in their POAs. On the molecular level, $C_6H_{10}O_5$ has the highest proportion (~7% to ~30%) in the POAs measured
446　by the EESI-TOF (except for the plastic bags burning), followed by $C_8H_{12}O_6$ with fractions of ~2% to ~9%. The
447　chemical composition measured with AMS covers a wide range of non-refractory organic and inorganic
448　components. However, the extensive fragmentation concentrates the measured mass-to-charge ratio below ~120
449　and limits its chemical resolution. The chemical groups used to deduce the composition of particles could originate
450　from different compounds, which impedes us from seeing the full picture. The formula-based mass spectrum from
451　the EESI-TOF overcomes this deficiency and thus reveals the detailed characteristics.
452　However, many compounds are present ubiquitously in all of the fuels used here, making it challenging to identify
453　atmospheric sources solely by visual comparisons of the full mass spectra. By using the Mann-Whitney U test to
454　identify potential markers among the studied fuels, we find that the markers identified by the AMS have greater
455　replicability and by EESI-TOF are more distinctive, thus providing an important reference for the source

456 apportionment. Overall, this work highlights the complex characteristics of POAs emitted from the burning of
457 solid fuels and proposes the markers for separating different sources using the AMS and EESI-TOF.
458 This work shows mass spectral profiles of burning emissions on bulk and molecular level, which improves our
459 understanding of POA from different fuels. The markers provided in this study are crucial for distinguishing the
460 sources of aerosols in the atmosphere and enhancing the interpretation of source apportionment. In the future, the
461 volatility and chemical reactivity of the proposed markers should be tested to determine their atmospheric stability
462 and their ability to be a robust marker. More burning fuels such as coal and grass could be conducted to enrich
463 the spectral database.
464 Future studies will probe the usefulness of these markers, if they are long lived enough in the atmosphere to
465 provide useful separation between complex emission sources shown here. This will either focus on online
466 measurements in polluted regions or from offline filter analysis from similar regions. Clearly, the dominant
467 biomass burning markers (levoglucosan and others) are not robust to be used to separate different biomass sources,
468 though they are robust for identification of general biomass burning aerosol. Nitrogen containing compounds
469 emitted from cow dung emissions can provide a very unique set of markers for separating this source from other
470 biomass sources. Additionally, resin acids from observed in the emissions from spruce and pine emissions provide
471 unique species associated with these emissions (and observed previously).
472 At the present moment, to provide insight into the usefulness of these markers within the context of ambient
473 measurements, or against source apportionment methods, we would require a robust dataset of comparable data
474 to test these markers and average emission profiles against.

475 **Data availability**

476 The datasets are available upon request to the corresponding authors.

477 **Author contributions**

478 JZ, TTW, KL, DMB, EG, KYC, and SB conducted the burning experiments. JZ analyzed the data and wrote the
479 manuscript. DSW, MS, TQC, LQ, and DB participated in the campaign. DMB, KL, IEH, HL, JGS, and ASHP
480 participated in the interpretation of data.

481 **Competing interests**

482 The authors declare that they have no conflict of interest.

483 **Disclaimer**

Reference

Adam, M. G., Tran, P. T. M., Bolan, N., and Balasubramanian, R.: Biomass burning-derived airborne particulate matter in Southeast Asia: A critical review, J Hazard Mater, 407, 124760, https://www.ncbi.nlm.nih.gov/pubmed/33341572, 2021.

Aiken, A. C., DeCarlo, P. F., and Jimenez, J. L.: Elemental Analysis of Organic Species with Electron Ionization High-Resolution Mass Spectrometry, Anal. Chem., 79, 8350-8358, https://doi.org/10.1021/ac071150w, 2007.

Alfarra, M. R., Prevot, A. S. H., Szidat, S., Sandradewi, J., Weimer, S., Lanz, V. A., Schreiber, D., Mohr, M., and Baltensperger, U.: Identification of the Mass Spectral Signature of Organic Aerosols from Wood Burning Emissions, Environmental Science & Technology, 41, 5770-5777, https://doi.org/10.1021/es062289b, 2007.

Andreae, M. O.: Emission of trace gases and aerosols from biomass burning – an updated assessment, Atmos. Chem. Phys., 19, 8523-8546, https://acp.copernicus.org/articles/19/8523/2019/, 2019.

Bahreini, R., Keywood, M. D., Ng, N. L., Varutbangkul, V., Gao, S., Flagan, R. C., Seinfeld, J. H., Worsnop, D. R., and Jimenez, J. L.: Measurements of Secondary Organic Aerosol from Oxidation of Cycloalkenes, Terpenes, and m-Xylene Using an Aerodyne Aerosol Mass Spectrometer, Environ. Sci. Technol., 39, 5674-5688, https://doi.org/10.1021/es048061a, 2005.

Bell, D. M., Wu, C., Bertrand, A., Graham, E., Schoonbaert, J., Giannoukos, S., Baltensperger, U., Prevot, A. S. H., Riipinen, I., El Haddad, I., and Mohr, C.: Particle-phase processing of α-pinene NO3 secondary organic aerosol in the dark, Atmos. Chem. Phys., 22, 13167-13182, https://acp.copernicus.org/articles/22/13167/2022/, 2022.

Bertrand, A., Stefenelli, G., Bruns, E. A., Pieber, S. M., Temime-Roussel, B., Slowik, J. G., Prévôt, A. S. H., Wortham, H., El Haddad, I., and Marchand, N.: Primary emissions and secondary aerosol production potential from woodstoves for residential heating: Influence of the stove technology and combustion efficiency, Atmos. Environ., 169, 65-79, https://www.sciencedirect.com/science/article/pii/S1352231017305861, 2017.

Bertrand, A., Stefenelli, G., Jen, C. N., Pieber, S. M., Bruns, E. A., Ni, H., Temime-Roussel, B., Slowik, J. G., Goldstein, A. H., El Haddad, I., Baltensperger, U., Prévôt, A. S. H., Wortham, H., and Marchand, N.: Evolution of the chemical fingerprint of biomass burning organic aerosol during aging, Atmos. Chem. Phys., 18, 7607-7624, https://acp.copernicus.org/articles/18/7607/2018/, 2018.

Bond, T. C., Bhardwaj, E., Dong, R., Jogani, R., Jung, S., Roden, C., Streets, D. G., and Trautmann, N. M.: Historical emissions of black and organic carbon aerosol from energy-related combustion, 1850–2000, Global Biogeochem. Cycles, 21, https://agupubs.onlinelibrary.wiley.com/doi/abs/10.1029/2006GB002840, 2007.

Brown, W. L., Day, D. A., Stark, H., Pagonis, D., Krechmer, J. E., Liu, X., Price, D. J., Katz, E. F., DeCarlo, P. F., Masoud, C. G., Wang, D. S., Hildebrandt Ruiz, L., Arata, C., Lunderberg, D. M., Goldstein, A. H., Farmer, D. K., Vance, M. E., and Jimenez, J. L.: Real-time organic aerosol chemical speciation in the indoor environment using extractive electrospray ionization mass spectrometry, Indoor Air, 31, 141-155, https://www.ncbi.nlm.nih.gov/pubmed/32696534, 2021.

Bruns, E. A., Slowik, J. G., El Haddad, I., Kilic, D., Klein, F., Dommen, J., Temime-Roussel, B., Marchand, N., Baltensperger, U., and Prévôt, A. S. H.: Characterization of gas-phase organics using proton transfer reaction time-of-flight mass spectrometry: fresh and aged residential wood combustion emissions, Atmos. Chem. Phys., 17, 705-720, https://acp.copernicus.org/articles/17/705/2017/, 2017.

Canagaratna, M. R., Jimenez, J. L., Kroll, J. H., Chen, Q., Kessler, S. H., Massoli, P., Hildebrandt Ruiz, L., Fortner, E., Williams, L. R., Wilson, K. R., Surratt, J. D., Donahue, N. M., Jayne, J. T., and Worsnop, D. R.: Elemental ratio measurements of organic compounds using aerosol mass spectrometry: characterization, improved calibration, and implications, Atmos. Chem. Phys., 15, 253-272, https://acp.copernicus.org/articles/15/253/2015/, 2015.

Census of India: Households by Availability of Separate Kitchen and Type of Fuel Used for Cooking, available 474 at: https://censusindia.gov.in/census.website/data/census-tables, 2011.

Chen, G., Sosedova, Y., Canonaco, F., Fröhlich, R., Tobler, A., Vlachou, A., Daellenbach, K. R., Bozzetti, C., Hueglin, C., Graf, P., Baltensperger, U., Slowik, J. G., El Haddad, I., and Prévôt, A. S. H.: Time-dependent source apportionment of submicron organic aerosol for a rural site in an alpine valley using a rolling positive matrix

14

factorisation (PMF) window, Atmos. Chem. Phys., 21, 15081-15101, https://acp.copernicus.org/articles/21/15081/2021/, 2021.

Chen, J., Li, C., Ristovski, Z., Milic, A., Gu, Y., Islam, M. S., Wang, S., Hao, J., Zhang, H., He, C., Guo, H., Fu, H., Miljevic, B., Morawska, L., Thai, P., Lam, Y. F., Pereira, G., Ding, A., Huang, X., and Dumka, U. C.: A review of biomass burning: Emissions and impacts on air quality, health and climate in China, Sci. Total Environ., 579, 1000-1034, https://www.sciencedirect.com/science/article/pii/S0048969716324561, 2017.

Colombini, M. P., Modugno, F., and Ribechini, E.: Direct exposure electron ionization mass spectrometry and gas chromatography/mass spectrometry techniques to study organic coatings on archaeological amphorae, J. Mass Spectrom., 40, 675-687, https://analyticalsciencejournals.onlinelibrary.wiley.com/doi/abs/10.1002/jms.841, 2005.

Crippa, M., Canonaco, F., Lanz, V. A., Äijälä, M., Allan, J. D., Carbone, S., Capes, G., Ceburnis, D., Dall'Osto, M., Day, D. A., DeCarlo, P. F., Ehn, M., Eriksson, A., Freney, E., Hildebrandt Ruiz, L., Hillamo, R., Jimenez, J. L., Junninen, H., Kiendler-Scharr, A., Kortelainen, A. M., Kulmala, M., Laaksonen, A., Mensah, A. A., Mohr, C., Nemitz, E., O'Dowd, C., Ovadnevaite, J., Pandis, S. N., Petäjä, T., Poulain, L., Saarikoski, S., Sellegri, K., Swietlicki, E., Tiitta, P., Worsnop, D. R., Baltensperger, U., and Prévôt, A. S. H.: Organic aerosol components derived from 25 AMS data sets across Europe using a consistent ME-2 based source apportionment approach, Atmos. Chem. Phys., 14, 6159-6176, https://acp.copernicus.org/articles/14/6159/2014/, 2014.

Cubison, M. J., Ortega, A. M., Hayes, P. L., Farmer, D. K., Day, D., Lechner, M. J., Brune, W. H., Apel, E., Diskin, G. S., Fisher, J. A., Fuelberg, H. E., Hecobian, A., Knapp, D. J., Mikoviny, T., Riemer, D., Sachse, G. W., Sessions, W., Weber, R. J., Weinheimer, A. J., Wisthaler, A., and Jimenez, J. L.: Effects of aging on organic aerosol from open biomass burning smoke in aircraft and laboratory studies, Atmos. Chem. Phys., 11, 12049-12064, https://acp.copernicus.org/articles/11/12049/2011/, 2011.

Daellenbach, K. R., Uzu, G., Jiang, J., Cassagnes, L.-E., Leni, Z., Vlachou, A., Stefenelli, G., Canonaco, F., Weber, S., Segers, A., Kuenen, J. J. P., Schaap, M., Favez, O., Albinet, A., Aksoyoglu, S., Dommen, J., Baltensperger, U., Geiser, M., El Haddad, I., Jaffrezo, J.-L., and Prévôt, A. S. H.: Sources of particulate-matter air pollution and its oxidative potential in Europe, Nature, 587, 414-419, https://doi.org/10.1038/s41586-020-2902-8, 2020.

de Oliveira Alves, N., Vessoni, A. T., Quinet, A., Fortunato, R. S., Kajitani, G. S., Peixoto, M. S., Hacon, S. d. S., Artaxo, P., Saldiva, P., Menck, C. F. M., and Batistuzzo de Medeiros, S. R.: Biomass burning in the Amazon region causes DNA damage and cell death in human lung cells, Sci. Rep., 7, 10937, https://doi.org/10.1038/s41598-017-11024-3, 2017.

DeCarlo, P. F., Kimmel, J. R., Trimborn, A., Northway, M. J., Jayne, J. T., Aiken, A. C., Gonin, M., Fuhrer, K., Horvath, T., Docherty, K. S., Worsnop, D. R., and Jimenez, J. L.: Field-Deployable, High-Resolution, Time-of-Flight Aerosol Mass Spectrometer, Anal. Chem., 78, 8281-8289, https://doi.org/10.1021/ac061249n, 2006.

Dzepina, K., Arey, J., Marr, L. C., Worsnop, D. R., Salcedo, D., Zhang, Q., Onasch, T. B., Molina, L. T., Molina, M. J., and Jimenez, J. L.: Detection of particle-phase polycyclic aromatic hydrocarbons in Mexico City using an aerosol mass spectrometer, Int. J. Mass Spectrom., 263, 152-170, https://doi.org/10.1016/j.ijms.2007.01.010, 2007.

Fang, Z., Deng, W., Zhang, Y., Ding, X., Tang, M., Liu, T., Hu, Q., Zhu, M., Wang, Z., Yang, W., Huang, Z., Song, W., Bi, X., Chen, J., Sun, Y., George, C., and Wang, X.: Open burning of rice, corn and wheat straws: primary emissions, photochemical aging, and secondary organic aerosol formation, Atmos. Chem. Phys., 17, 14821-14839, https://doi.org/10.5194/acp-17-14821-2017, 2017.

Farmer, D. K., Matsunaga, A., Docherty, K. S., Surratt, J. D., Seinfeld, J. H., Ziemann, P. J., and Jimenez, J. L.: Response of an aerosol mass spectrometer to organonitrates and organosulfates and implications for atmospheric chemistry, Proc Natl Acad Sci U S A, 107, 6670-6675, https://www.ncbi.nlm.nih.gov/pubmed/20194777, 2010.

Favez, O., El Haddad, I., Piot, C., Boréave, A., Abidi, E., Marchand, N., Jaffrezo, J. L., Besombes, J. L., Personnaz, M. B., Sciare, J., Wortham, H., George, C., and D'Anna, B.: Inter-comparison of source apportionment models for the estimation of wood burning aerosols during wintertime in an Alpine city (Grenoble, France), Atmos. Chem. Phys., 10, 5295-5314, https://acp.copernicus.org/articles/10/5295/2010/, 2010.

Fleming, L. T., Lin, P., Laskin, A., Laskin, J., Weltman, R., Edwards, R. D., Arora, N. K., Yadav, A., Meinardi, S., Blake, D. R., Pillarisetti, A., Smith, K. R., and Nizkorodov, S. A.: Molecular composition of particulate matter emissions from dung and brushwood burning household cookstoves in Haryana, India, Atmos. Chem. Phys., 18, 2461-2480, https://acp.copernicus.org/articles/18/2461/2018/, 2018.

Font-Palma, C.: Methods for the Treatment of Cattle Manure—A Review, C, 5, http://doi.org/10.3390/c5020027, 2019.

Goetz, J. D., Giordano, M. R., Stockwell, C. E., Christian, T. J., Maharjan, R., Adhikari, S., Bhave, P. V., Praveen, P. S., Panday, A. K., Jayarathne, T., Stone, E. A., Yokelson, R. J., and DeCarlo, P. F.: Speciated online PM1 from South Asian combustion sources – Part 1: Fuel-based emission factors and size distributions, Atmos. Chem. Phys., 18, 14653-14679, https://acp.copernicus.org/articles/18/14653/2018/, 2018.

Haque, M. M., Kawamura, K., Deshmukh, D. K., Fang, C., Song, W., Mengying, B., and Zhang, Y. L.: Characterization of organic aerosols from a Chinese megacity during winter: predominance of fossil fuel combustion, Atmos. Chem. Phys., 19, 5147-5164, https://acp.copernicus.org/articles/19/5147/2019/, 2019.

15

Hennigan, C. J., Miracolo, M. A., Engelhart, G. J., May, A. A., Presto, A. A., Lee, T., Sullivan, A. P., McMeeking, G. R., Coe, H., Wold, C. E., Hao, W. M., Gilman, J. B., Kuster, W. C., de Gouw, J., Schichtel, B. A., Collett, J. L., Kreidenweis, S. M., and Robinson, A. L.: Chemical and physical transformations of organic aerosol from the photo-oxidation of open biomass burning emissions in an environmental chamber, Atmos. Chem. Phys., 11, 7669-7686, https://acp.copernicus.org/articles/11/7669/2011/, 2011.

Hoffer, A., Jancsek-Turóczi, B., Tóth, Á., Kiss, G., Naghiu, A., Levei, E. A., Marmureanu, L., Machon, A., and Gelencsér, A.: Emission factors for PM10 and polycyclic aromatic hydrocarbons (PAHs) from illegal burning of different types of municipal waste in households, Atmos. Chem. Phys., 20, 16135-16144, https://acp.copernicus.org/articles/20/16135/2020/, 2020.

Holmbom, B.: Improved gas chromatographic analysis of fatty and resin acid mixtures with special reference to tall oil, J. Am. Oil Chem. Soc., 54, 289-293, https://aocs.onlinelibrary.wiley.com/doi/abs/10.1007/BF02671098, 1977.

Huang, R. J., Zhang, Y., Bozzetti, C., Ho, K. F., Cao, J. J., Han, Y., Daellenbach, K. R., Slowik, J. G., Platt, S. M., Canonaco, F., Zotter, P., Wolf, R., Pieber, S. M., Bruns, E. A., Crippa, M., Ciarelli, G., Piazzalunga, A., Schwikowski, M., Abbaszade, G., Schnelle-Kreis, J., Zimmermann, R., An, Z., Szidat, S., Baltensperger, U., El Haddad, I., and Prevot, A. S.: High secondary aerosol contribution to particulate pollution during haze events in China, Nature, 514, 218-222, https://www.ncbi.nlm.nih.gov/pubmed/25231863, 2014.

Islam, M. R., Welker, J., Salam, A., and Stone, E. A.: Plastic Burning Impacts on Atmospheric Fine Particulate Matter at Urban and Rural Sites in the USA and Bangladesh, ACS Environ. Au, https://doi.org/10.1021/acsenvironau.1c00054 https://pubs.acs.org/doi/pdf/10.1021/acsenvironau.1c00054, 2022.

Jayarathne, T., Stockwell, C. E., Bhave, P. V., Praveen, P. S., Rathnayake, C. M., Islam, M. R., Panday, A. K., Adhikari, S., Maharjan, R., Goetz, J. D., DeCarlo, P. F., Saikawa, E., Yokelson, R. J., and Stone, E. A.: Nepal Ambient Monitoring and Source Testing Experiment (NAMaSTE): emissions of particulate matter from wood- and dung-fueled cooking fires, garbage and crop residue burning, brick kilns, and other sources, Atmos. Chem. Phys., 18, 2259-2286, 2018.

Jen, C. N., Hatch, L. E., Selimovic, V., Yokelson, R. J., Weber, R., Fernandez, A. E., Kreisberg, N. M., Barsanti, K. C., and Goldstein, A. H.: Speciated and total emission factors of particulate organics from burning western US wildland fuels and their dependence on combustion efficiency, Atmos. Chem. Phys., 19, 1013-1026, https://acp.copernicus.org/articles/19/1013/2019/, 2019.

Ji, X., Le Bihan, O., Ramalho, O., Mandin, C., D'Anna, B., Martinon, L., Nicolas, M., Bard, D., and Pairon, J. C.: Characterization of particles emitted by incense burning in an experimental house, Indoor Air, 20, 147-158, https://www.ncbi.nlm.nih.gov/pubmed/20409193, 2010.

Kong, X., Salvador, C. M., Carlsson, S., Pathak, R., Davidsson, K. O., Le Breton, M., Gaita, S. M., Mitra, K., Hallquist, A. M., Hallquist, M., and Pettersson, J. B. C.: Molecular characterization and optical properties of primary emissions from a residential wood burning boiler, Sci Total Environ, 754, 142143, https://www.ncbi.nlm.nih.gov/pubmed/32898781, 2021.

Kumar, V., Giannoukos, S., Haslett, S. L., Tong, Y., Singh, A., Bertrand, A., Lee, C. P., Wang, D. S., Bhattu, D., Stefenelli, G., Dave, J. S., Puthussery, J. V., Qi, L., Vats, P., Rai, P., Casotto, R., Satish, R., Mishra, S., Pospisilova, V., Mohr, C., Bell, D. M., Ganguly, D., Verma, V., Rastogi, N., Baltensperger, U., Tripathi, S. N., Prévôt, A. S. H., and Slowik, J. G.: Highly time-resolved chemical speciation and source apportionment of organic aerosol components in Delhi, India, using extractive electrospray ionization mass spectrometry, Atmos. Chem. Phys., 22, 7739-7761, https://acp.copernicus.org/articles/22/7739/2022/, 2022.

Li, C.-T., Zhuang, H.-K., Hsieh, L.-T., Lee, W.-J., and Tsao, M.-C.: PAH emission from the incineration of three plastic wastes, Environ. Int., 27, 61-67, https://www.sciencedirect.com/science/article/pii/S0160412001000563, 2001.

Li, X., Wang, S., Duan, L., Hao, J., Li, C., Chen, Y., and Yang, L.: Particulate and Trace Gas Emissions from Open Burning of Wheat Straw and Corn Stover in China, Environ. Sci. Technol., 41, 6052-6058, https://doi.org/10.1021/es0705137, 2007.

Li, Y.-C. and Kuo, Y.-H.: Labdane-type diterpenoids from the wood of Cunninghamia konishii, Chemical & pharmaceutical bulletin, 50, 498-500, https://doi.org/10.1248/cpb.50.498, 2002.

Liang, Y., Jen, C. N., Weber, R. J., Misztal, P. K., and Goldstein, A. H.: Chemical composition of PM2.5 in October 2017 Northern California wildfire plumes, Atmos. Chem. Phys., 21, 5719-5737, https://acp.copernicus.org/articles/21/5719/2021/, 2021.

Løkke, H.: Picein and piceol concentrations in Norway spruce, Ecotoxicology and Environmental Safety, 19, 301-309, https://www.sciencedirect.com/science/article/pii/014765139090032Z, 1990.

Lopez-Hilfiker, F. D., Pospisilova, V., Huang, W., Kalberer, M., Mohr, C., Stefenelli, G., Thornton, J. A., Baltensperger, U., Prevot, A. S. H., and Slowik, J. G.: An extractive electrospray ionization time-of-flight mass spectrometer (EESI-TOF) for online measurement of atmospheric aerosol particles, Atmos. Meas. Tech., 12, 4867-4886, https://doi.org/10.5194/amt-12-4867-2019, 2019.

Lopez-Hilfiker, F. D., Mohr, C., Ehn, M., Rubach, F., Kleist, E., Wildt, J., Mentel, T. F., Lutz, A., Hallquist, M., Worsnop, D., and Thornton, J. A.: A novel method for online analysis of gas and particle composition: description and evaluation of a Filter Inlet for Gases and AEROsols (FIGAERO), Atmos. Meas. Tech., 7, 983-1001, https://amt.copernicus.org/articles/7/983/2014/, 2014.

Mann, H. B. and Whitney, D. R.: On a test of whether one of two random variables is stochastically larger than the other, Annals of Mathematical Statistics, 18, 50-60, https://doi.org/10.1214/aoms/1177730491, 1947.

Mofikoya, O. O., Mäkinen, M., and Jänis, J.: Chemical Fingerprinting of Conifer Needle Essential Oils and Solvent Extracts by Ultrahigh-Resolution Fourier Transform Ion Cyclotron Resonance Mass Spectrometry, ACS Omega, 5, 10543-10552, https://doi.org/10.1021/acsomega.0c00901, 2020.

Mohr, C., DeCarlo, P. F., Heringa, M. F., Chirico, R., Slowik, J. G., Richter, R., Reche, C., Alastuey, A., Querol, X., Seco, R., Peñuelas, J., Jiménez, J. L., Crippa, M., Zimmermann, R., Baltensperger, U., and Prévôt, A. S. H.: Identification and quantification of organic aerosol from cooking and other sources in Barcelona using aerosol mass spectrometer data, Atmos. Chem. Phys., 12, 1649-1665, https://acp.copernicus.org/articles/12/1649/2012/, 2012.

Neves, L., Ferreira, V., and Oliveira, R.: Co-composting cow manure with food waste: The influence of lipids content, https://doi.org/10.1016/j.biortech.2008.10.030, 2009a.

Neves, L., Oliveira, R., and Alves, M. M.: Fate of LCFA in the co-digestion of cow manure, food waste and discontinuous addition of oil, Water Res., 43, 5142-5150, https://www.sciencedirect.com/science/article/pii/S0043135409005168, 2009b.

Ng, N. L., Canagaratna, M. R., Zhang, Q., Jimenez, J. L., Tian, J., Ulbrich, I. M., Kroll, J. H., Docherty, K. S., Chhabra, P. S., Bahreini, R., Murphy, S. M., Seinfeld, J. H., Hildebrandt, L., Donahue, N. M., DeCarlo, P. F., Lanz, V. A., Prévôt, A. S. H., Dinar, E., Rudich, Y., and Worsnop, D. R.: Organic aerosol components observed in Northern Hemispheric datasets from Aerosol Mass Spectrometry, Atmos. Chem. Phys., 10, 4625-4641, https://acp.copernicus.org/articles/10/4625/2010/, 2010.

Pathak, G., Nichter, M., Hardon, A., Moyer, E., Latkar, A., Simbaya, J., Pakasi, D., Taqueban, E., and Love, J.: Plastic pollution and the open burning of plastic wastes, Global Environ. Change, 80, 2023.

Qi, L., Bozzetti, C., Corbin, J. C., Daellenbach, K. R., El Haddad, I., Zhang, Q., Wang, J., Baltensperger, U., Prevot, A. S. H., Chen, M., Ge, X., and Slowik, J. G.: Source identification and characterization of organic nitrogen in atmospheric aerosols at a suburban site in China, Sci Total Environ, 818, 151800, https://www.ncbi.nlm.nih.gov/pubmed/34813816, 2022.

Radke, L. and Ward, D., Crutzen, P. J., and Goldammer, J. G. (Eds.): The Ecological, Atmospheric, and Climatic Importance of Vegetation Fires., Environmental Sciences Research Report, John Wiley and Sons, Inc., New York, pp.1993.

Rugiel, M. M., Setkowicz, Z. K., Drozdz, A. K., Janeczko, K. J., Kutorasińska, J., and Chwiej, J. G.: The Use of Fourier Transform Infrared Microspectroscopy for the Determination of Biochemical Anomalies of the Hippocampal Formation Characteristic for the Kindling Model of Seizures, ACS Chem. Neurosci., 12, 4564-4579, https://doi.org/10.1021/acschemneuro.1c00642, 2021.

Saiz-Jimenez, C. and De Leeuw, J. W.: Lignin pyrolysis products: Their structures and their significance as biomarkers, Org. Geochem., 10, 869-876, https://www.sciencedirect.com/science/article/pii/S0146638086800249, 1986.

Simoneit, B. R. T.: Biomass burning — a review of organic tracers for smoke from incomplete combustion, Appl. Geochem., 17, 129-162, https://www.sciencedirect.com/science/article/pii/S0883292701000610, 2002.

Simoneit, B. R. T., Rogge, W. F., Mazurek, M. A., Standley, L. J., Hildemann, L. M., and Cass, G. R.: Lignin pyrolysis products, lignans, and resin acids as specific tracers of plant classes in emissions from biomass combustion, Environ. Sci. Technol., 27, 2533-2541, https://doi.org/10.1021/es00048a034, 1993.

Smith, K. R., Bruce, N., Balakrishnan, K., Adair-Rohani, H., Balmes, J., Chafe, Z., Dherani, M., Hosgood, H. D., Mehta, S., Pope, D., and Rehfuess, E.: Millions Dead: How Do We Know and What Does It Mean? Methods Used in the Comparative Risk Assessment of Household Air Pollution, Annu. Rev. Public Health, 35, 185-206, https://www.annualreviews.org/doi/abs/10.1146/annurev-publhealth-032013-182356, 2014.

Stark, H., Yatavelli, R. L. N., Thompson, S. L., Kang, H., Krechmer, J. E., Kimmel, J. R., Palm, B. B., Hu, W., Hayes, P. L., Day, D. A., Campuzano-Jost, P., Canagaratna, M. R., Jayne, J. T., Worsnop, D. R., and Jimenez, J. L.: Impact of Thermal Decomposition on Thermal Desorption Instruments: Advantage of Thermogram Analysis for Quantifying Volatility Distributions of Organic Species, Environ Sci Technol, 51, 8491-8500, https://www.ncbi.nlm.nih.gov/pubmed/28644613, 2017.

Stockwell, C. E., Christian, T. J., Goetz, J. D., Jayarathne, T., Bhave, P. V., Praveen, P. S., Adhikari, S., Maharjan, R., DeCarlo, P. F., Stone, E. A., Saikawa, E., Blake, D. R., Simpson, I. J., Yokelson, R. J., and Panday, A. K.: Nepal Ambient Monitoring and Source Testing Experiment (NAMaSTE): emissions of trace gases and light-absorbing carbon from wood and dung cooking fires, garbage and crop residue burning, brick kilns, and other sources, Atmos. Chem. Phys., 16, 11043-11081, https://acp.copernicus.org/articles/16/11043/2016/, 2016.

17

Surdu, M., Lamkaddam, H., Wang, D. S., Bell, D. M., Xiao, M., Lee, C. P., Li, D., Caudillo, L., Marie, G., Scholz, W., Wang, M., Lopez, B., Piedehierro, A. A., Ataei, F., Baalbaki, R., Bertozzi, B., Bogert, P., Brasseur, Z., Dada, L., Duplissy, J., Finkenzeller, H., He, X. C., Hohler, K., Korhonen, K., Krechmer, J. E., Lehtipalo, K., Mahfouz, N. G. A., Manninen, H. E., Marten, R., Massabo, D., Mauldin, R., Petaja, T., Pfeifer, J., Philippov, M., Rorup, B., Simon, M., Shen, J., Umo, N. S., Vogel, F., Weber, S. K., Zauner-Wieczorek, M., Volkamer, R., Saathoff, H., Mohler, O., Kirkby, J., Worsnop, D. R., Kulmala, M., Stratmann, F., Hansel, A., Curtius, J., Welti, A., Riva, M., Donahue, N. M., Baltensperger, U., and El Haddad, I.: Molecular Understanding of the Enhancement in Organic Aerosol Mass at High Relative Humidity, Environ Sci Technol, 57, 2297-2309, https://www.ncbi.nlm.nih.gov/pubmed/36716278, 2023.

Szmigielski, R., Surratt, J. D., Gómez-González, Y., Van der Veken, P., Kourtchev, I., Vermeylen, R., Blockhuys, F., Jaoui, M., Kleindienst, T. E., Lewandowski, M., Offenberg, J. H., Edney, E. O., Seinfeld, J. H., Maenhaut, W., and Claeys, M.: 3-methyl-1,2,3-butanetricarboxylic acid: An atmospheric tracer for terpene secondary organic aerosol, Geophys. Res. Lett., 34, https://agupubs.onlinelibrary.wiley.com/doi/abs/10.1029/2007GL031338, 2007.

Tai, K. Y., Dhaliwal, J., and Balasubramaniam, V.: Leveraging Mann–Whitney U test on large-scale genetic variation data for analysing malaria genetic markers, Malar. J., 21, 79, https://doi.org/10.1186/s12936-022-04104-x, 2022.

Tissari, J., Lyyränen, J., Hytönen, K., Sippula, O., Tapper, U., Frey, A., Saarnio, K., Pennanen, A. S., Hillamo, R., Salonen, R. O., Hirvonen, M. R., and Jokiniemi, J.: Fine particle and gaseous emissions from normal and smouldering wood combustion in a conventional masonry heater, Atmos. Environ., 42, 7862-7873, 2008.

Tobler, A., Bhattu, D., Canonaco, F., Lalchandani, V., Shukla, A., Thamban, N. M., Mishra, S., Srivastava, A. K., Bisht, D. S., Tiwari, S., Singh, S., Močnik, G., Baltensperger, U., Tripathi, S. N., Slowik, J. G., and Prévôt, A. S. H.: Chemical characterization of PM2.5 and source apportionment of organic aerosol in New Delhi, India, Sci. Total Environ., 745, 140924, https://www.sciencedirect.com/science/article/pii/S0048969720344533, 2020.

Tong, Y., Pospisilova, V., Qi, L., Duan, J., Gu, Y., Kumar, V., Rai, P., Stefenelli, G., Wang, L., Wang, Y., Zhong, H., Baltensperger, U., Cao, J., Huang, R. J., Prévôt, A. S. H., and Slowik, J. G.: Quantification of solid fuel combustion and aqueous chemistry contributions to secondary organic aerosol during wintertime haze events in Beijing, Atmos. Chem. Phys., 21, 9859-9886, https://acp.copernicus.org/articles/21/9859/2021/, 2021.

Tuet, W. Y., Liu, F., de Oliveira Alves, N., Fok, S., Artaxo, P., Vasconcellos, P., Champion, J. A., and Ng, N. L.: Chemical Oxidative Potential and Cellular Oxidative Stress from Open Biomass Burning Aerosol, Environ. Sci. Technol. Lett., 6, 126-132, https://doi.org/10.1021/acs.estlett.9b00060, 2019.

Wang, Y., Wang, Q., Ye, J., Yan, M., Qin, Q., Prévôt, A. S. H., and Cao, J.: A Review of Aerosol Chemical Composition and Sources in Representative Regions of China during Wintertime, Atmosphere, 10, 277, https://www.mdpi.com/2073-4433/10/5/277, 2019.

Ward, D. E. and Hardy, C. C.: Smoke emissions from wildland fires, Environ. Int., 17, 117-134, https://www.sciencedirect.com/science/article/pii/0160412091900958, 1991.

Wilcoxon, F.: Individual Comparisons by Ranking Methods, Biometrics Bulletin, 1, 80-83, http://www.jstor.org/stable/3001968, 1945.

Wiyono, B., Tachibana, S., and Tinambunan, D.: Chemical Compositions of Pine Resin, Rosin and Turpentine Oil from West Java, Indonesian Journal of Forestry Research, 3, 7-17, http://doi.org/10.20886/ijfr.2006.3.1.7-17, 2006.

Wu, D., Li, Q., Shang, X., Liang, Y., Ding, X., Sun, H., Li, S., Wang, S., Chen, Y., and Chen, J.: Commodity plastic burning as a source of inhaled toxic aerosols, J Hazard Mater, 416, 125820, https://www.ncbi.nlm.nih.gov/pubmed/33887570, 2021.

Xu, W., He, Y., Qiu, Y., Chen, C., Xie, C., Lei, L., Li, Z., Sun, J., Li, J., Fu, P., Wang, Z., Worsnop, D. R., and Sun, Y.: Mass spectral characterization of primary emissions and implications in source apportionment of organic aerosol, Atmos. Meas. Tech., 13, 3205-3219, https://amt.copernicus.org/articles/13/3205/2020/, 2020.

Yee, L. D., Kautzman, K. E., Loza, C. L., Schilling, K. A., Coggon, M. M., Chhabra, P. S., Chan, M. N., Chan, A. W. H., Hersey, S. P., Crounse, J. D., Wennberg, P. O., Flagan, R. C., and Seinfeld, J. H.: Secondary organic aerosol formation from biomass burning intermediates: phenol and methoxyphenols, Atmos. Chem. Phys., 13, 8019-8043, https://acp.copernicus.org/articles/13/8019/2013/, 2013.

Zetra, Y., B. Sosrowidjojo, I., and Perry Burhan, R. Y.: AROMATIC BIOMARKER FROM BROWN COAL, SANGATTA COALFIELD, EAST BORNEO OF MIDDLE MIOCENE TO LATE MIOCENE AGE, Jurnal Teknologi, 78, https://journals.utm.my/jurnalteknologi/article/view/8822, 2016.

Zhang, J., Wang, X., Li, R., Dong, S., Chen, J., Zhang, Y., Zheng, P., Li, M., Chen, T., Liu, Y., Xue, L., Zhou, X., Du, L., Zhang, Q., and Wang, W.: Significant impacts of anthropogenic activities on monoterpene and oleic acid-derived particulate organic nitrates in the North China Plain, Atmos. Res., 256, 2021.

Zhou, H., Wu, C., Onwudili, J. A., Meng, A., Zhang, Y., and Williams, P. T.: Polycyclic aromatic hydrocarbons (PAH) formation from the pyrolysis of different municipal solid waste fractions, Waste Manag, 36, 136-146, https://www.ncbi.nlm.nih.gov/pubmed/25312776, 2015.

18

779
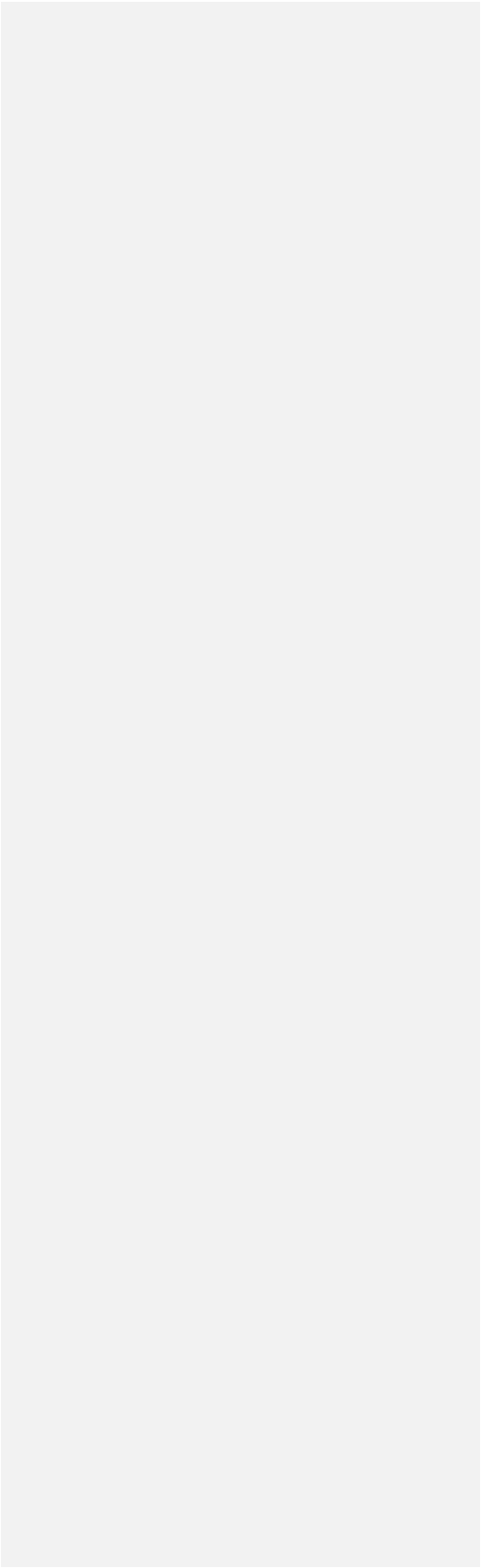
Tables and figures

781   **Table 1 Average emission factors of CO, CO₂, THC, PM, OM, and BC as well as MCE for 6 types of burning.**

Burning type	Carbon content	Particle density (g cm⁻³)	MCE	Emission factors (g kg⁻¹ fuel)					
				CO	CO₂	THC	PM	OM	eBC*
beech logs stove (n=5)	0.46	1.70	0.91±0.03	85.8±25.9	1466.9±65.8	19.3±5.5	7.6±2.2	6.2±2.8	2.43±0.9
spruce and pine logs stove (n=8)	0.46	1.70	0.91±0.02	83.8±26.7	1640.7±58	16.1±4.8	4.9±2.2	2.0±1.3	n.a
spruce and pine branches and needles open (n=4)	0.46	1.70	0.93±0.02	63.5±6.8	1668.9±26.7	14.1±3.4	9.4±2.7	3.8±1.1	n.a
straw open (n=6)	0.45	1.50	0.95±0.04	44.4±34.1	1511.7±103.2	19.1±17	2.8±1.2	2.4±1.3	0.7±0.2
cow dung open (n=6)	0.45	1.54	0.87±0.03	92.3±27.4	1366.2±88.4	30.3±8.5	16.6±10.8	16.2±10.8	0.8±0.3
plastic bags open** (n=4)	0.84	0.45	0.98±0.02	29.3±39.2	2956.6±138.9	18.2±28.6	3.1 2.7±1.3 2	1.1 3±0.3	1.0±0.3

782

783   *The number of burns is indicated by n. BC data is not available for some burns.

784   **The emission factors of PM and OM are corrected as explained in Supplement.

785

786

787
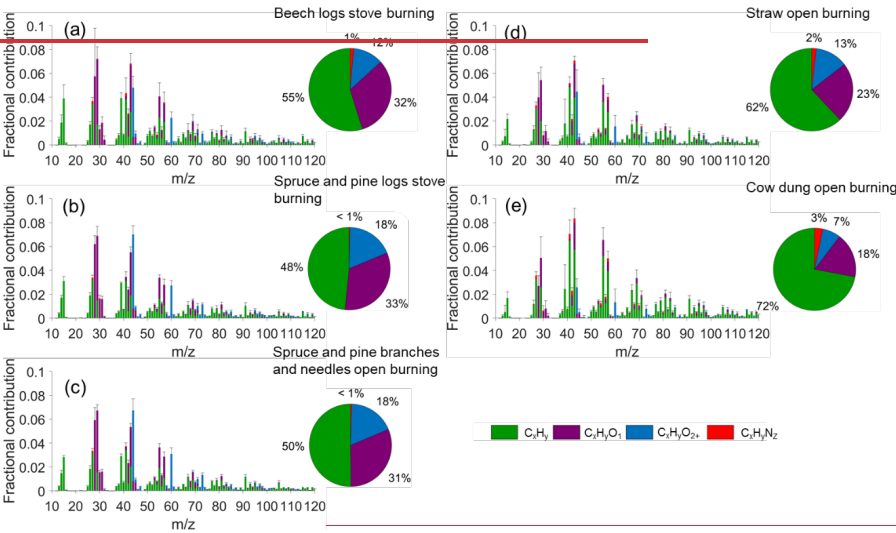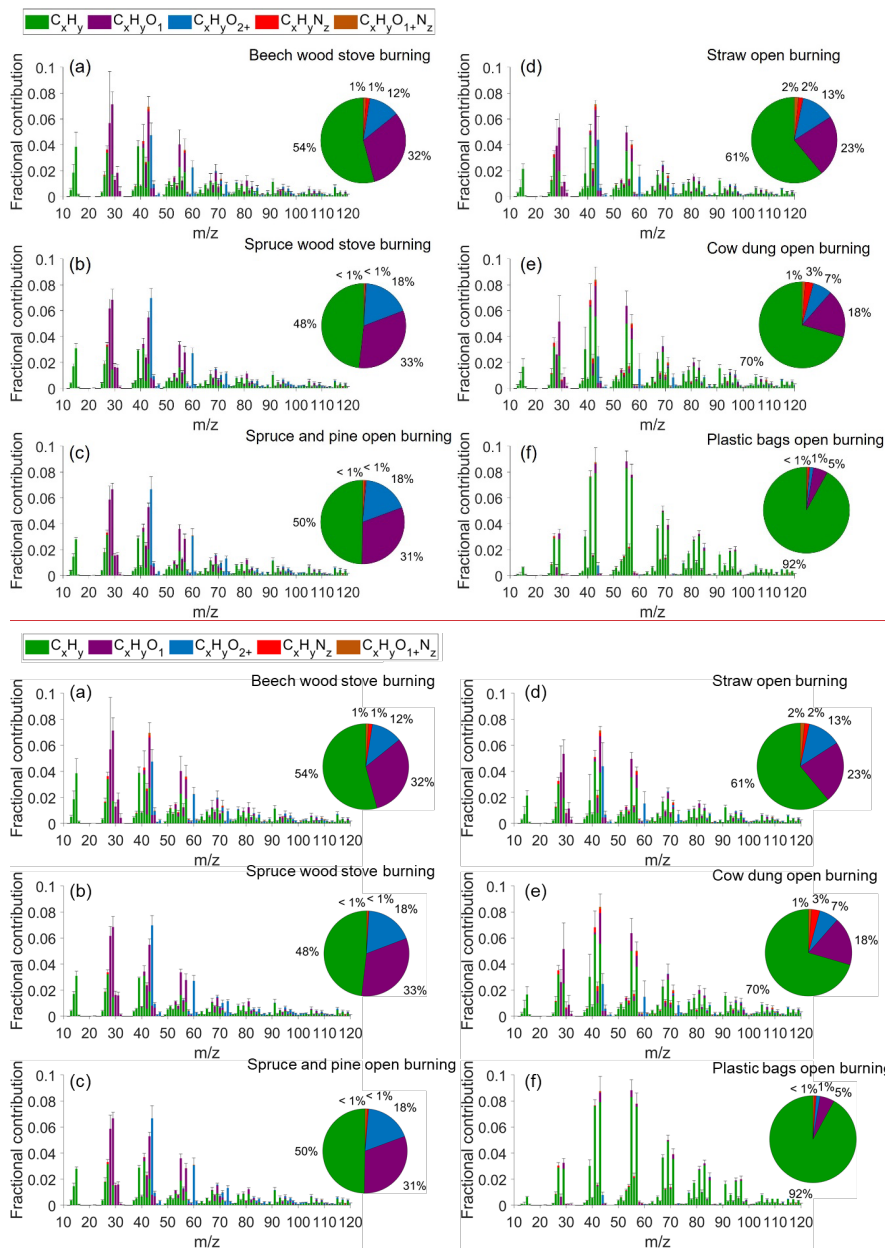
788 **Figure 1 Average AMS POA mass spectral profiles and elemental compositions of (a) beech logs stove burning (n=6; n**
789 **is the number of experiments), (b) spruce and pine logs stove burning (n=9), (c) spruce and pine branches and needles**
790 **open burning (n=4), (d) straw open burning (n=6), ~~and~~ (e) cow dung open burning (n=5), and (f) plastic bags burning**
791 **(n=4). The error bar denotes half standard deviation in grey. The pie chart showing the contribution of elemental**
792 **families is at the right of the mass spectrum.**
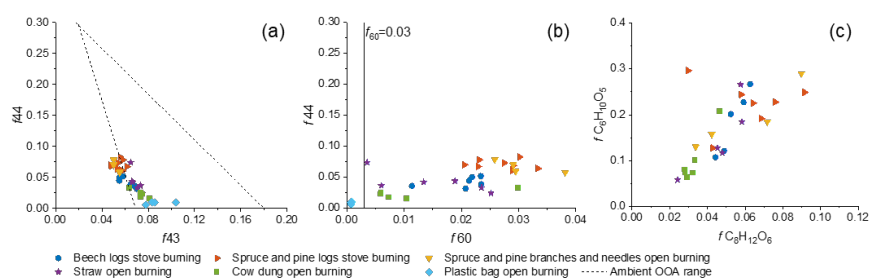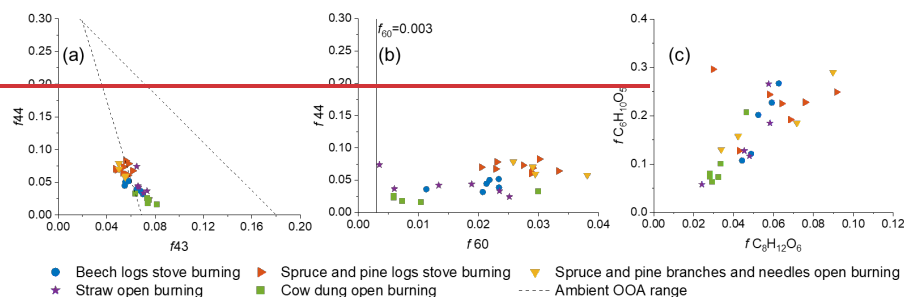
Figure 2. Scatter plots of (a) f_{44} vs. f_{43} from AMS, (b) f_{44} vs. f_{60} from AMS, and (c) $f C_6H_{10}O_5$ vs. $f C_8H_{12}O_6$ from EESI-TOF. The dashed line denotes the estimated OOA range and the solid line denotes f_{60} background level in the ambient from Ng et al. (2010) and Cubison et al. (2011).
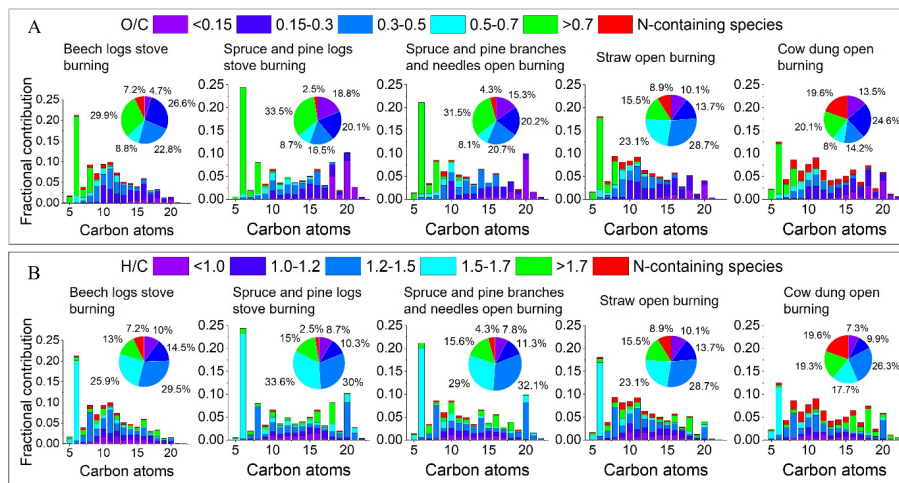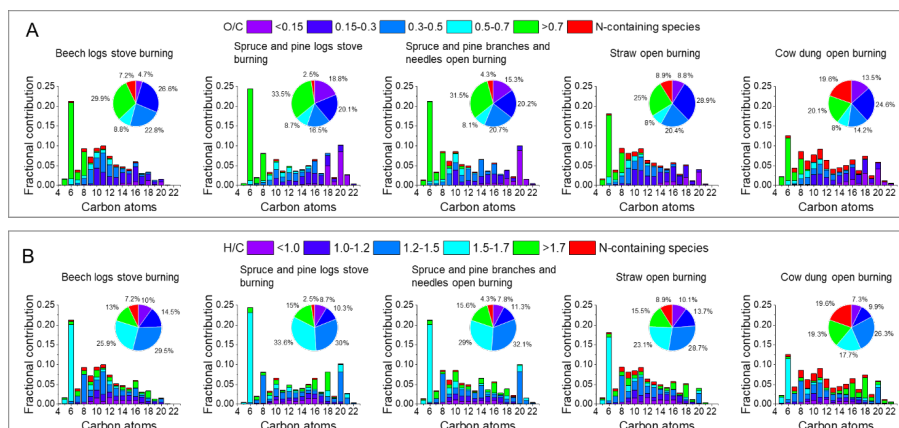
Figure 3 The average carbon and oxygen distribution colored by the O/C and H/C for non-N-containing species in panel A and B respectively with EESI-TOF. The N-containing species are colored in red. The pie charts are the corresponding contribution of a range of O/C or H/C ratios.

23
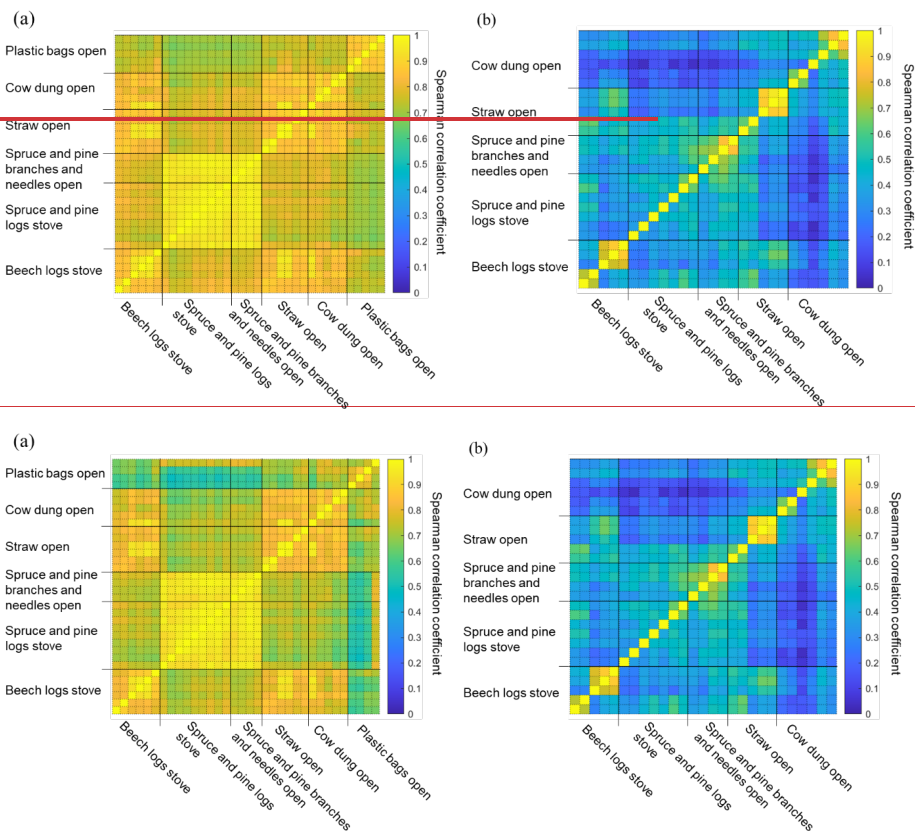
Figure 4 The correlation matrix of POAs measured with (a) the HR data from AMS and (b) EESI-TOF using Spearman correlation function. Note that some experiments did not have either AMS or EESI-TOF data.
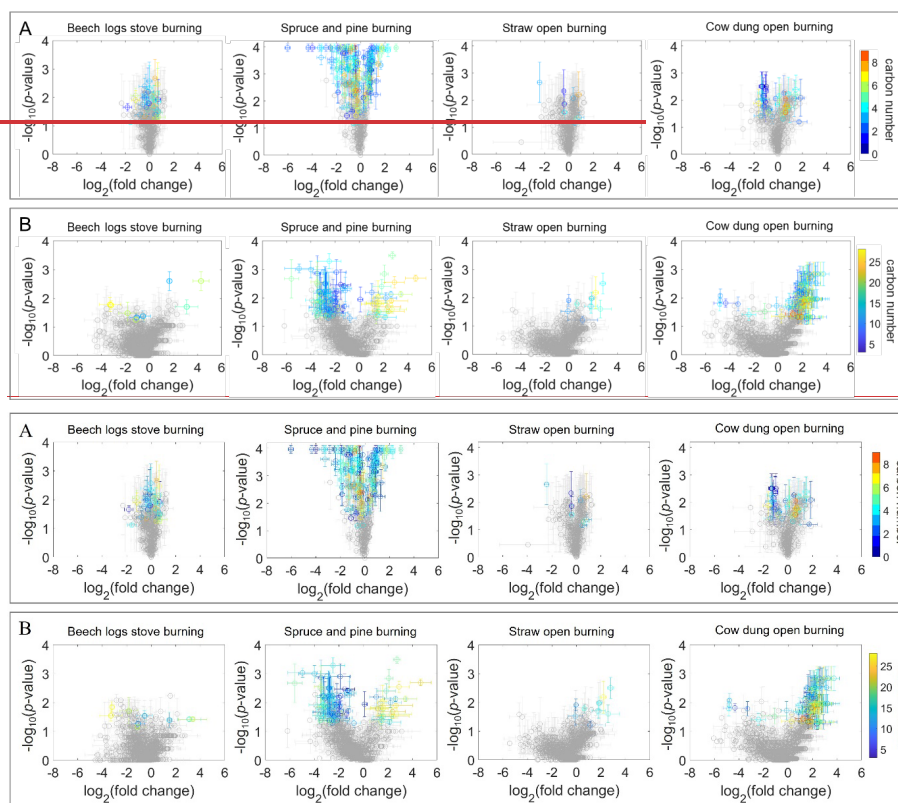
Figure 5 The statistic static *p*-value vs. fold change with the dataset from AMS in panel A and EESI-TOF in panel B. The color bars are the number of carbon atoms. The horizontal error bars are the 1 standard deviation given by the *p*-value variations in the pairwise tests, and the vertical error bars are the 1 standard deviation of the log$_2$(fold change).
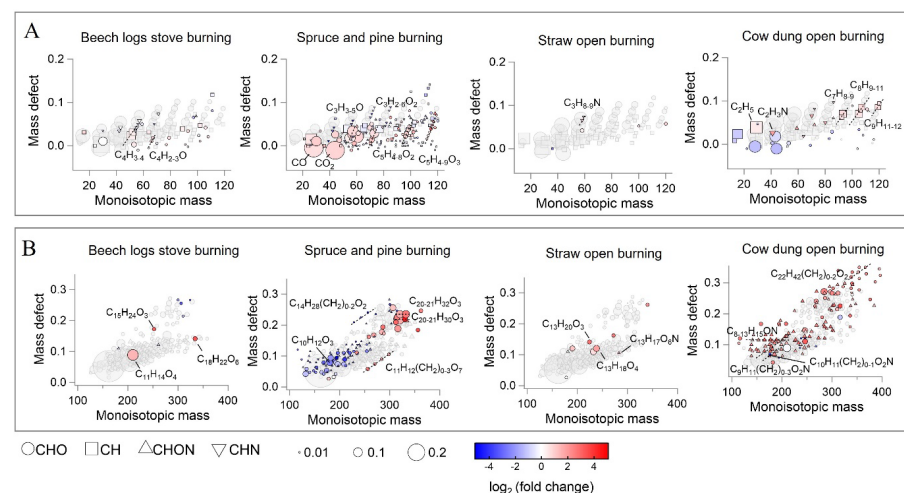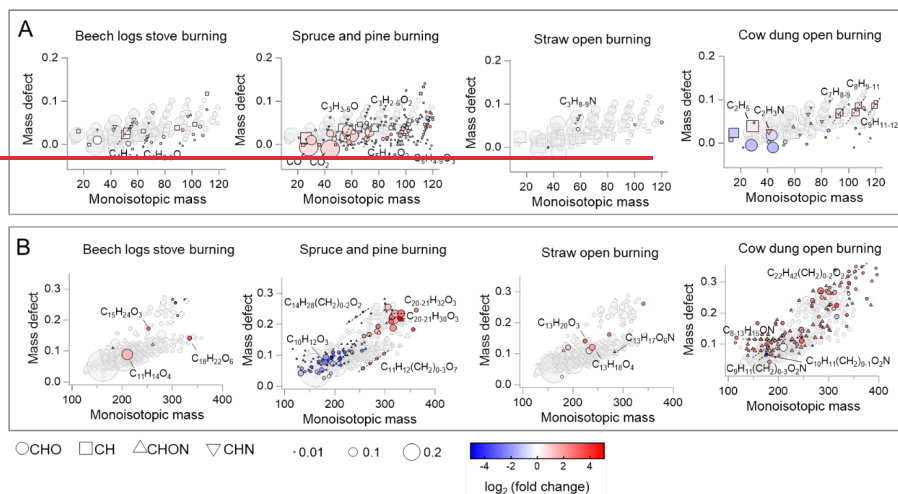
Figure 6 The mass defect plot with the dataset from AMS in panel A and EESI-TOF in panel B. The markers denotes the fragments or molecules having the same formula. They are sized by the square root of fractional contribution and colored by the $\log_2$(fold change).